On-surface synthesis

N-heterocyclic carbenes formation and dimerization

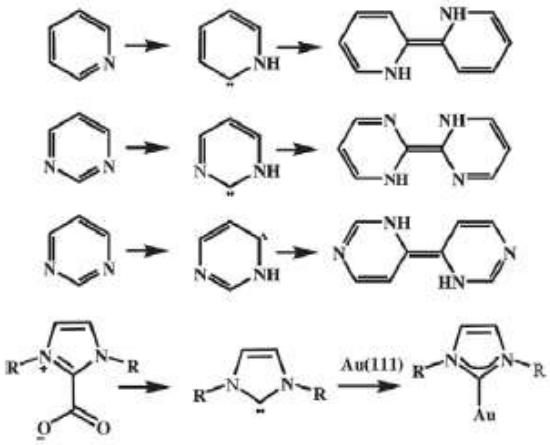

Glaser coupling

Alkyne cyclotrimerization

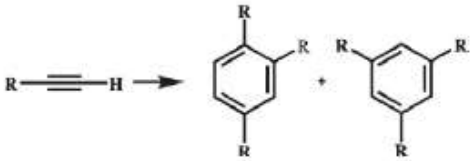

Metalated carbyne

Bergman reaction

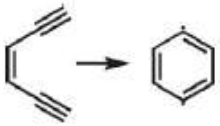

Azide–alkyne cycloaddition

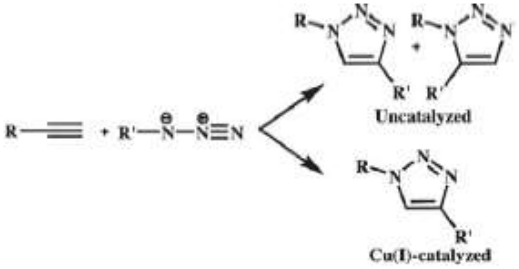

Sonogashira coupling

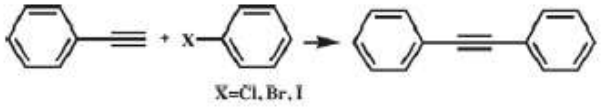

Nano Today 13 (2017) 77–96

Dehalogenative homocoupling of terminal alkynyl bromides	
Ullmann coupling	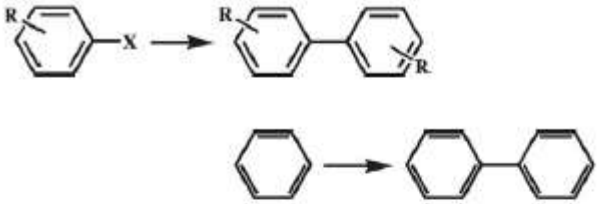
Aryl–aryl dehydrogenation coupling	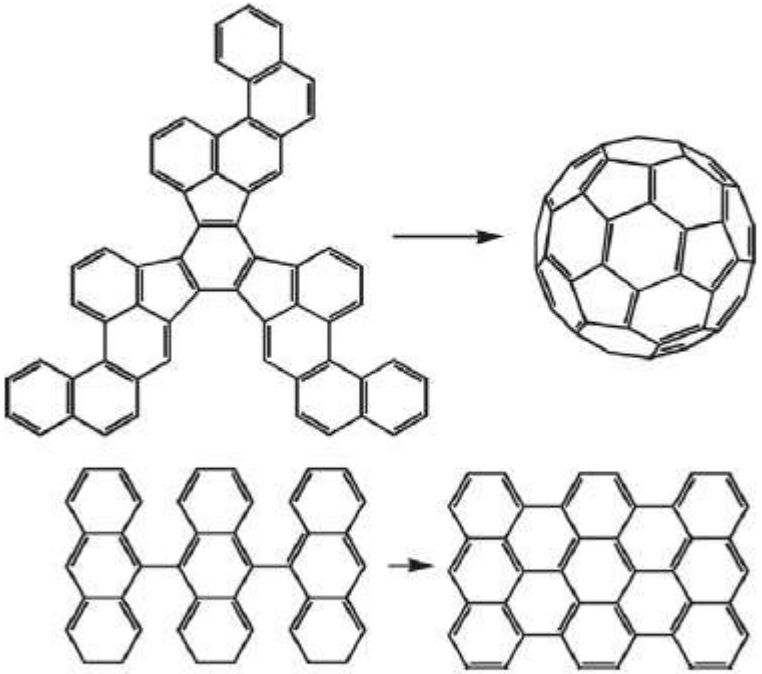
Dehydrogenative homocoupling of terminal alkene	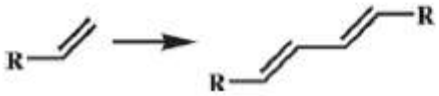

Dehalogenative homocoupling of terminal alkenyl bromides	
Diels–Alder reaction	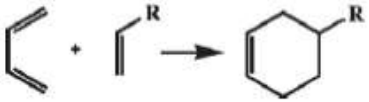
Wurtz coupling	
Linear alkane polymerization	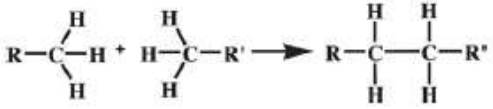
Decarboxylative polymerization	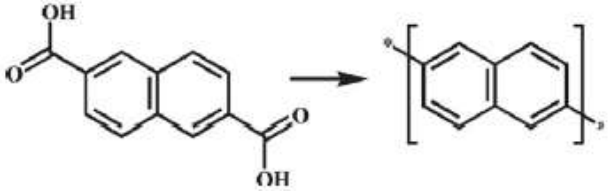
Dehydrogenative coupling	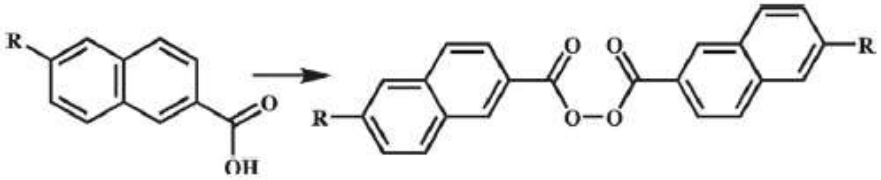
Dimerization and cyclotrimerization of acetyls	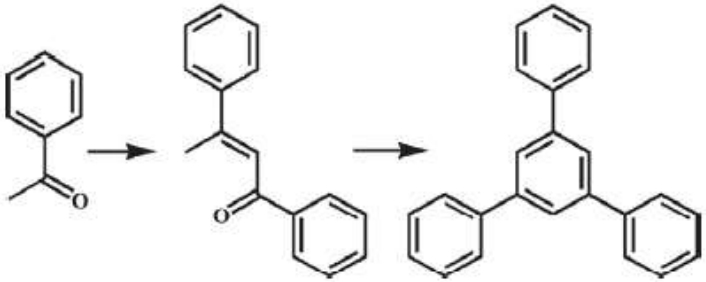
Dealkylation of ethers to alcohols	
Reduction	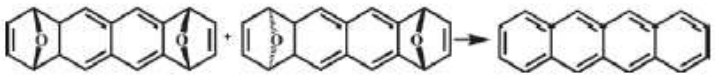

Schiff-base reaction (imine formation)

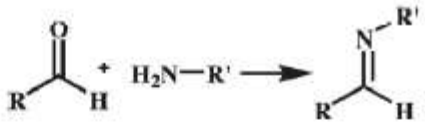

Boronic acid condensation

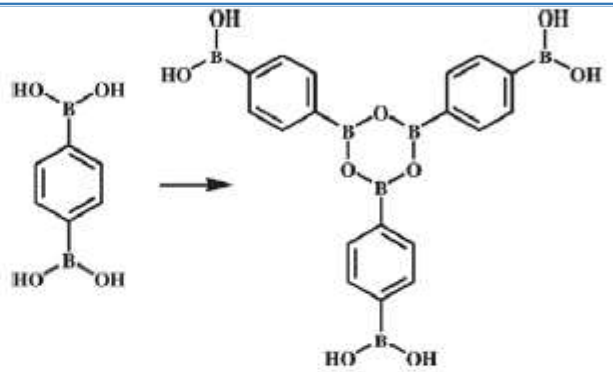

Surface confined
Metal–organic coordination

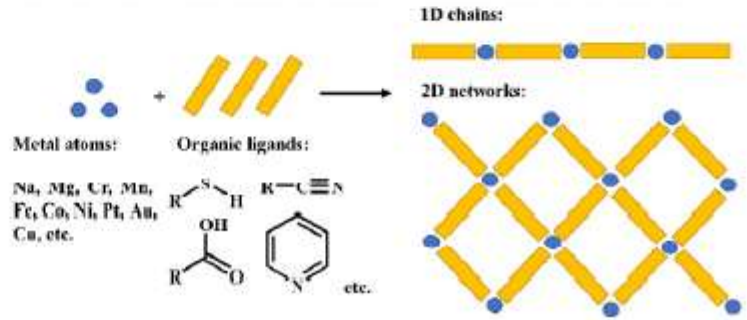

Reazione di Ullmann o Ullmann coupling

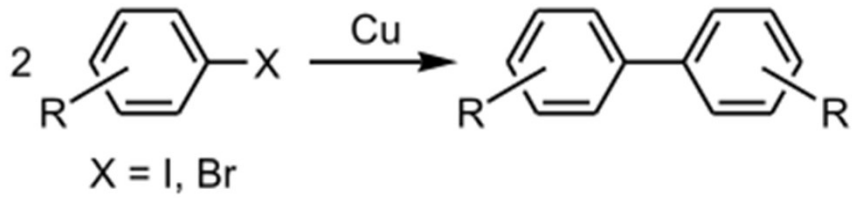

X alogeni, tipicamente Br

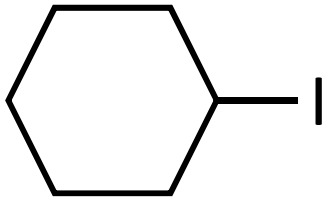

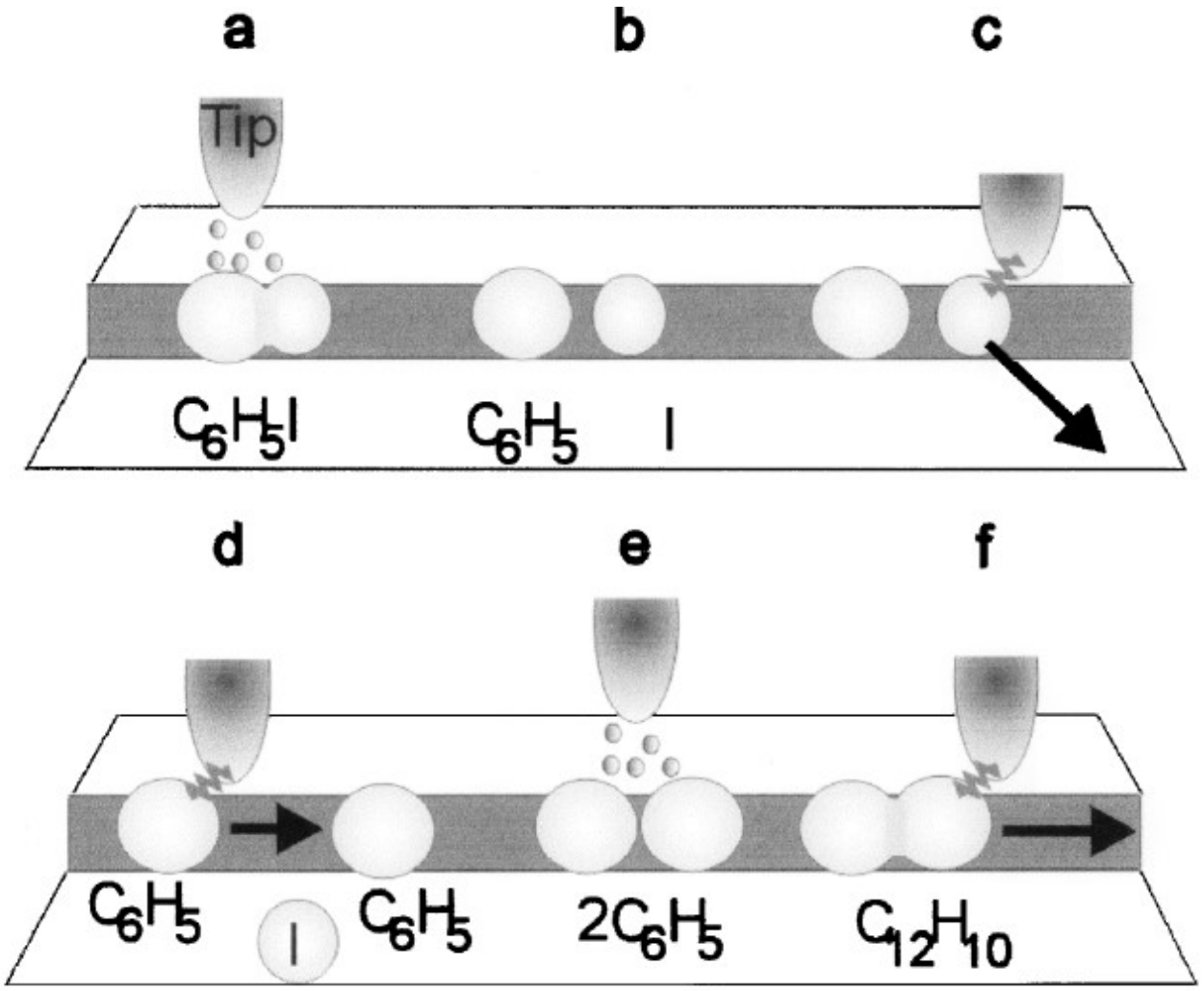

VOLUME 85, NUMBER 13 PHYSICAL REVIEW LETTERS 25 SEPTEMBER 2000

Inducing All Steps of a Chemical Reaction with the Scanning Tunneling Microscope Tip: Towards Single Molecule Engineering

Saw-Wai Hla,[1,2,*] Ludwig Bartels,[1,†] Gerhard Meyer,[1] and Karl-Heinz Rieder[1]

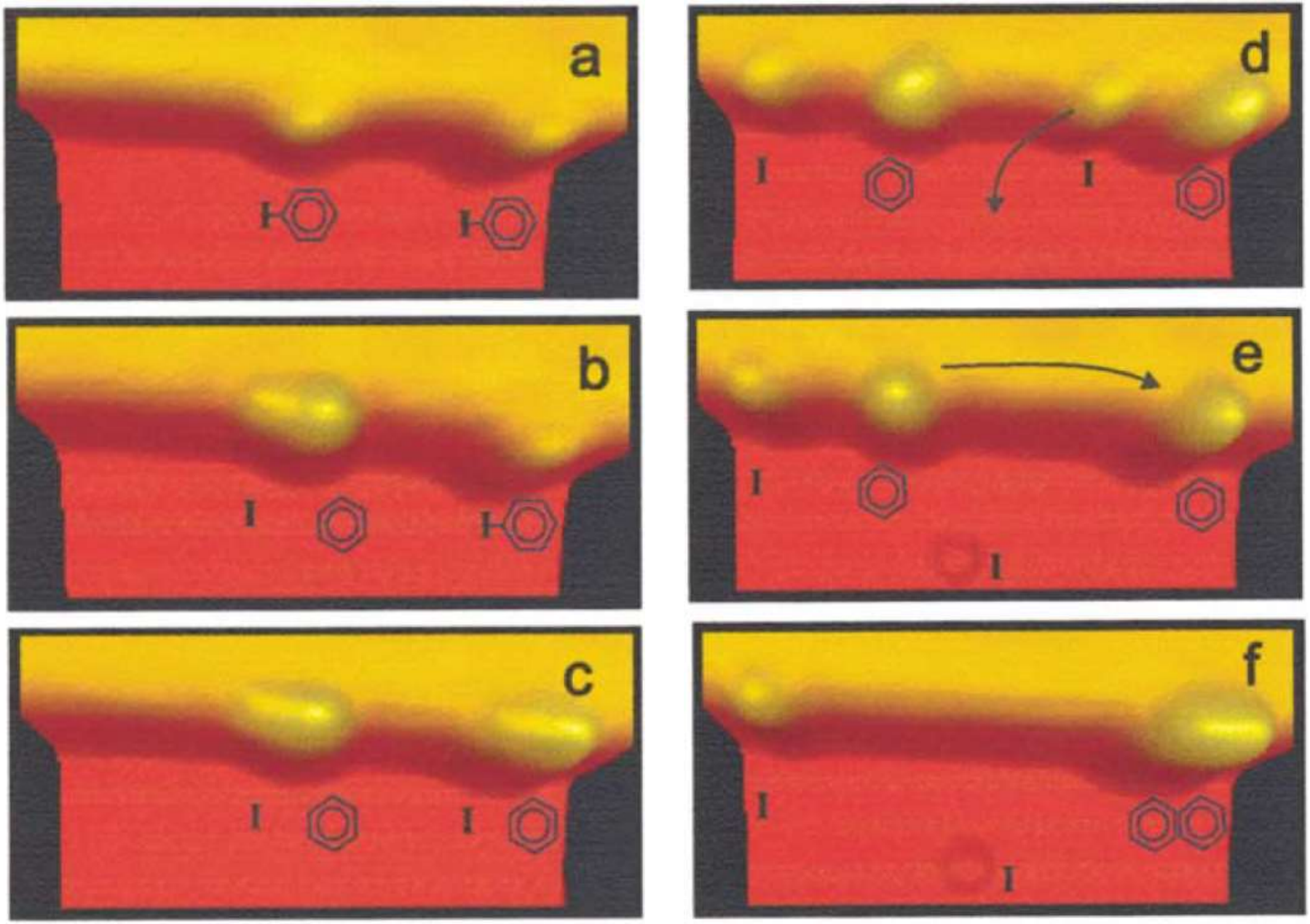
a
b
c
d
e
f

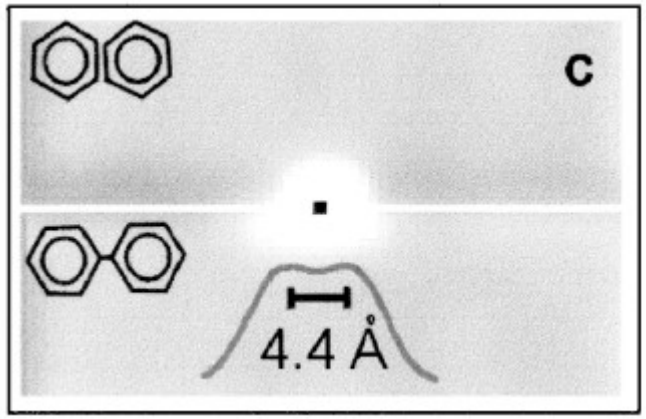
c
4.4 Å


a

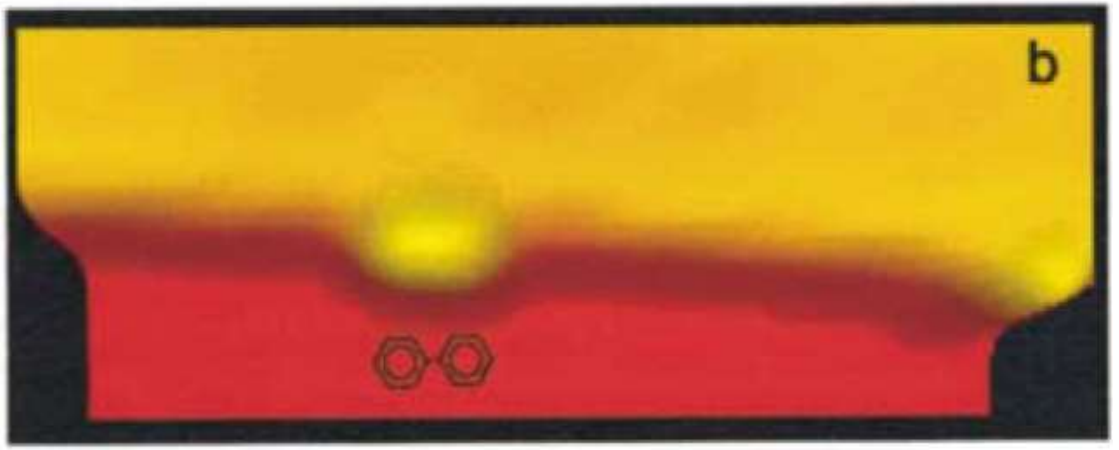
b

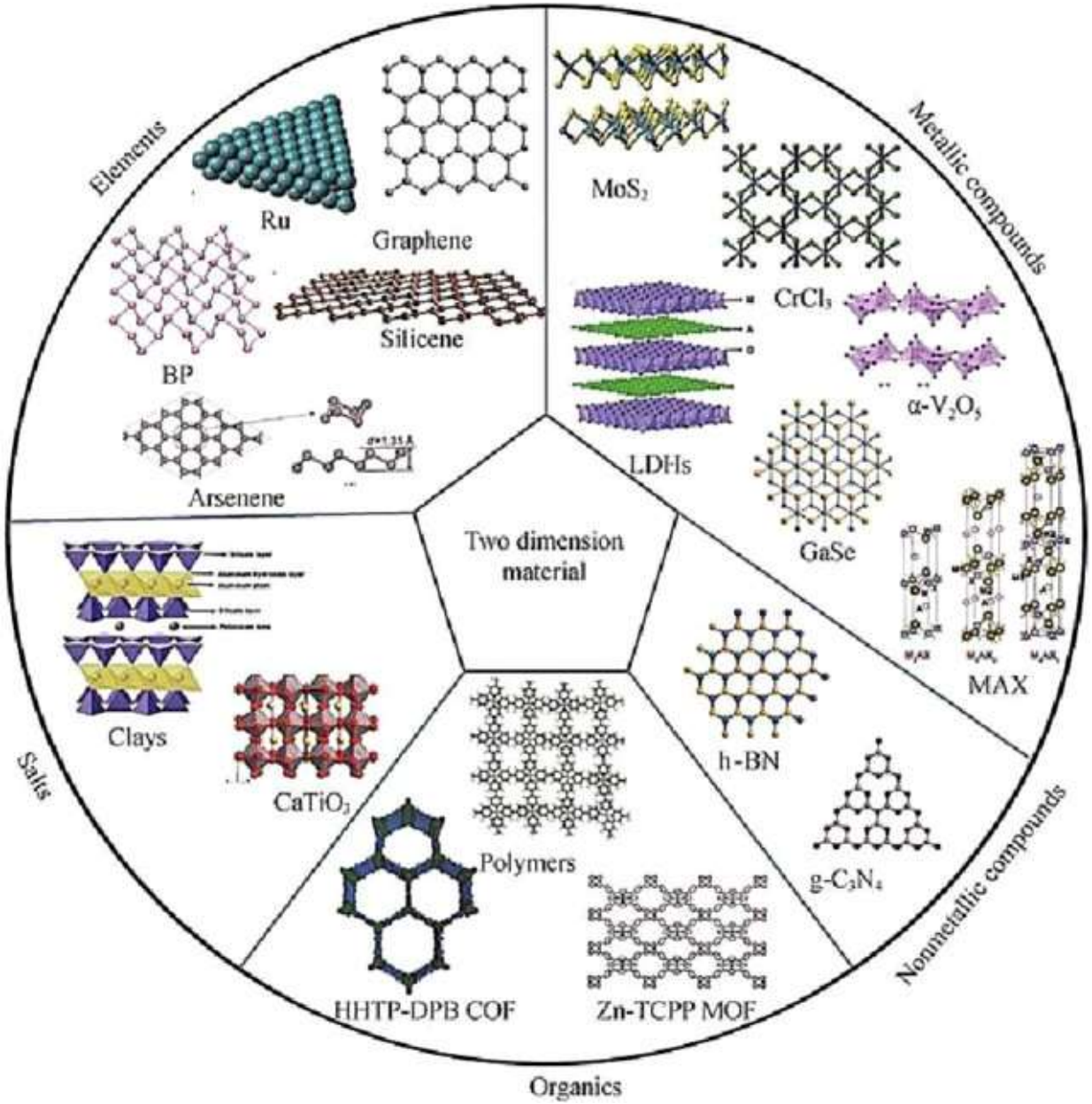

https://doi.org/10.1142/S1793292019300019

Covalent Organic Frameworks

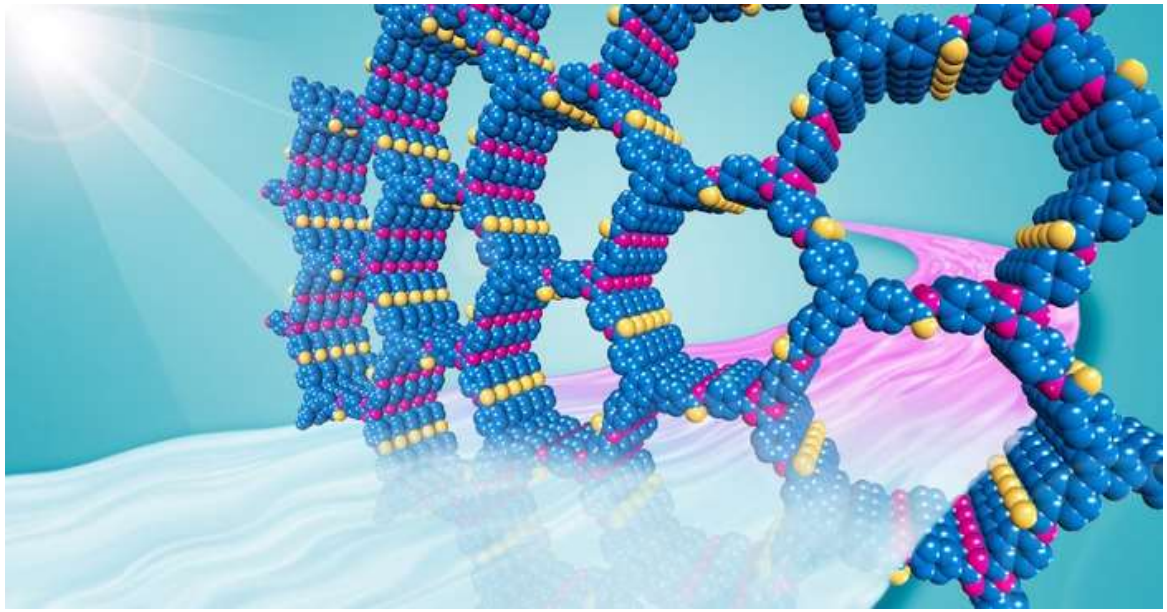

Storaging

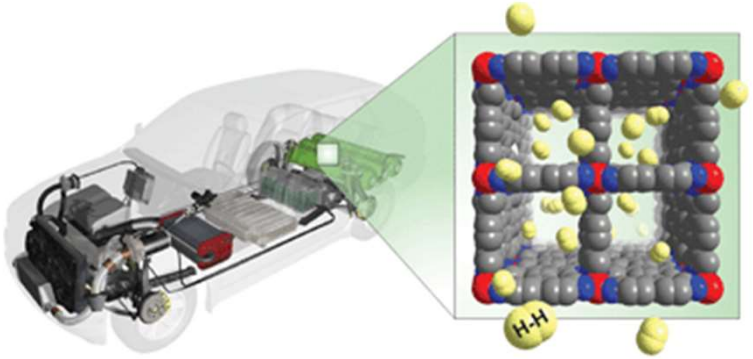

Fotocatalisi

La struttura del precursore determina la morfologia del 2D e la concentrazione di difetti

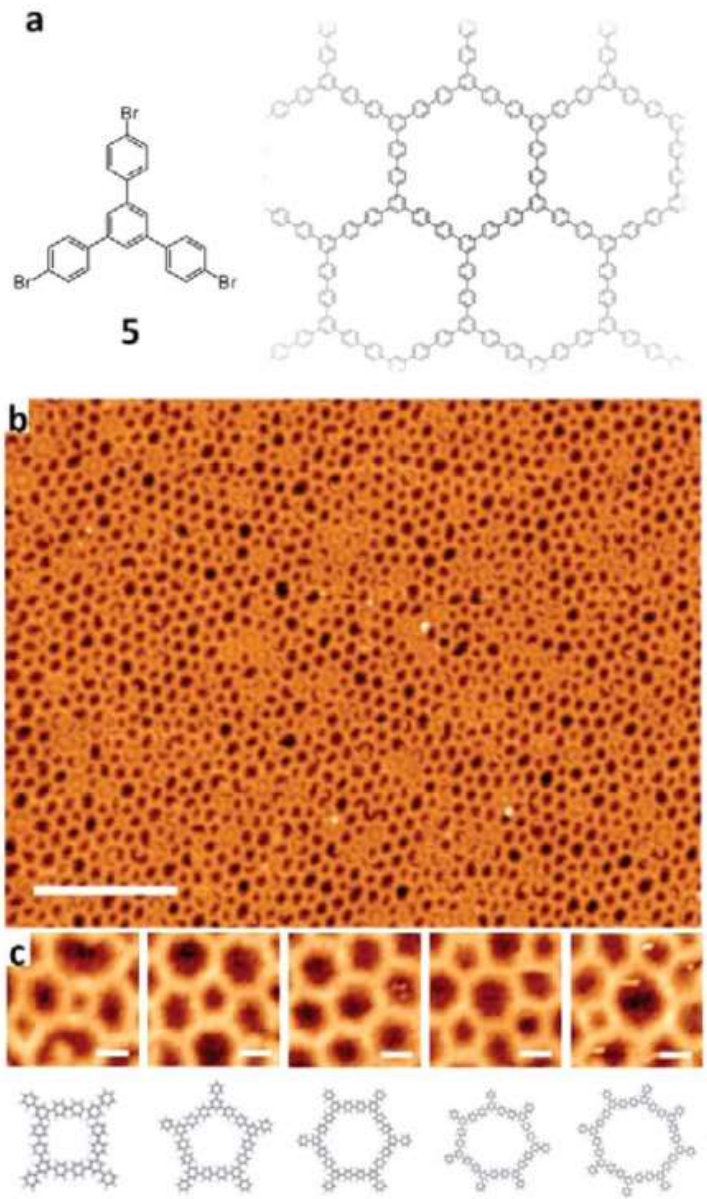

2D - COVALENT ORGANIC FRAMEWORK

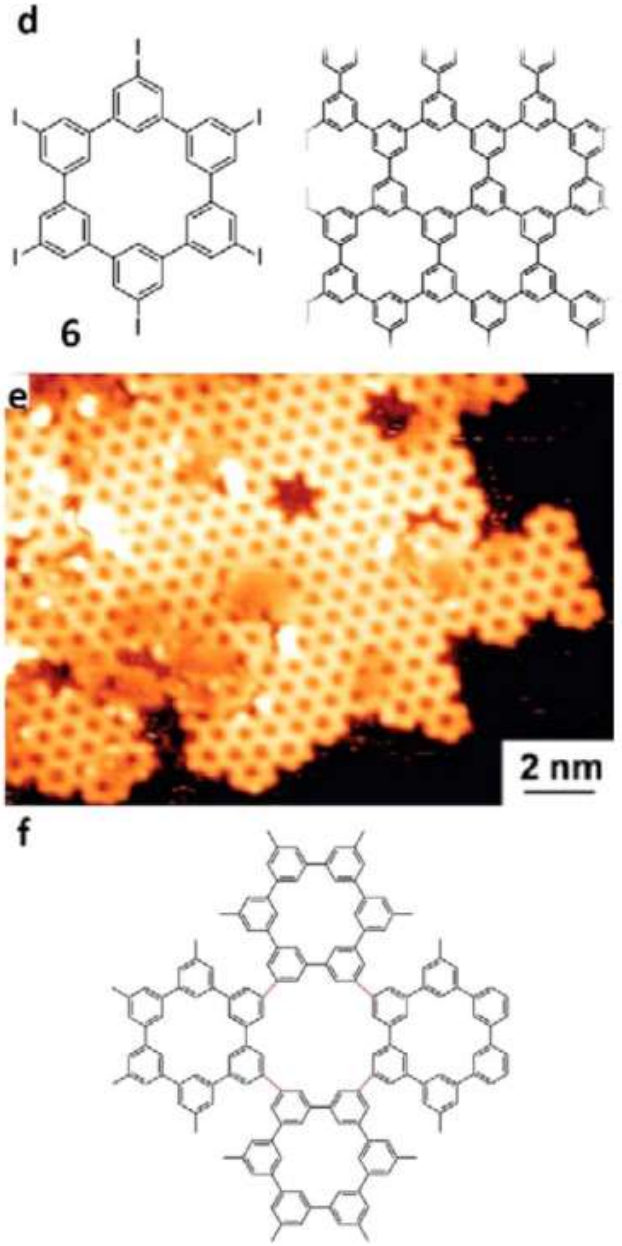

ACS Nano 2014, 8, 7880−7889.

Chem. Commun. 2010, 46, 7157−7159.

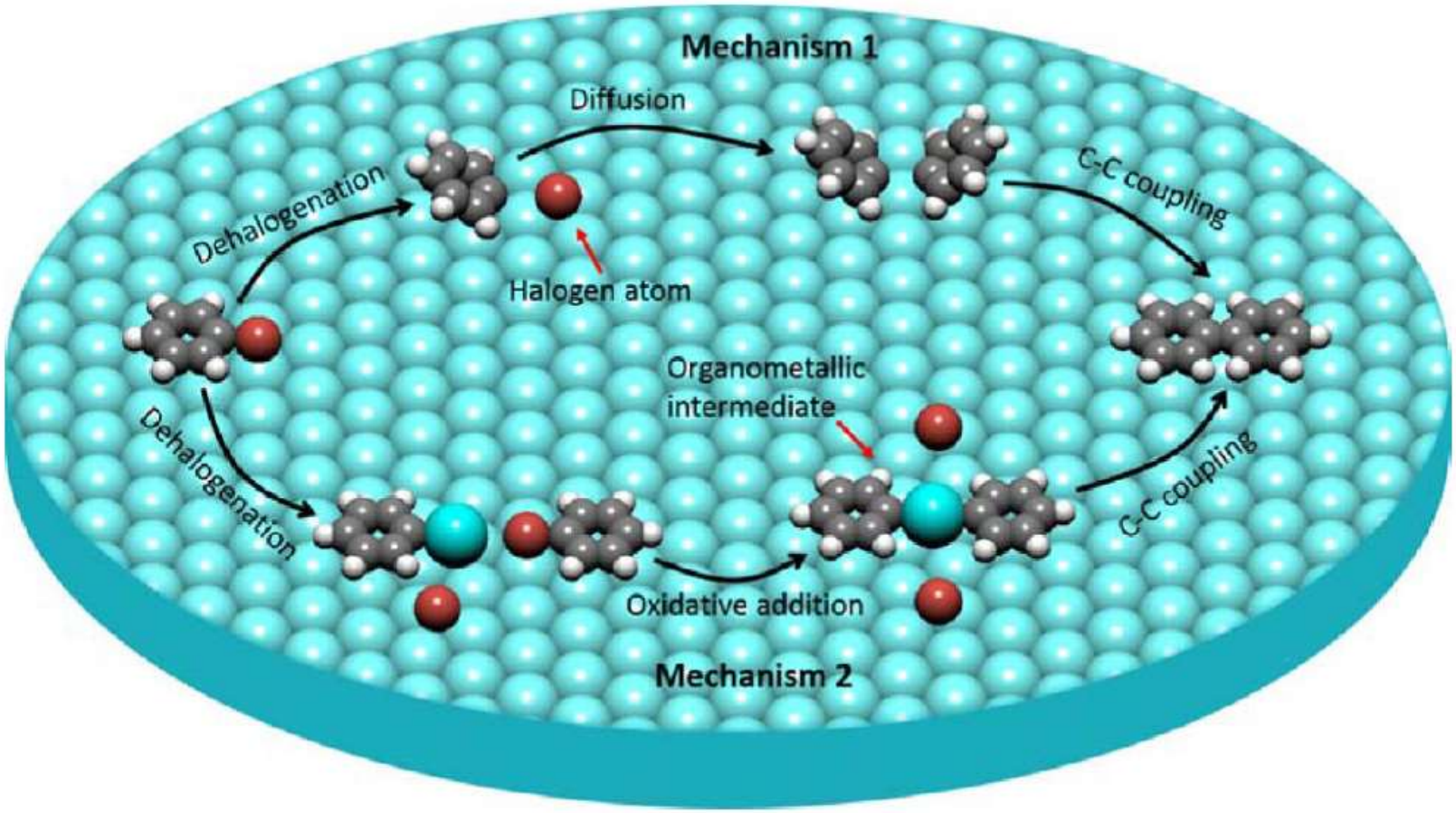

DOI: 10.1021/acs.accounts.5b00168
Acc. Chem. Res. 2015, 48, 2484−2494

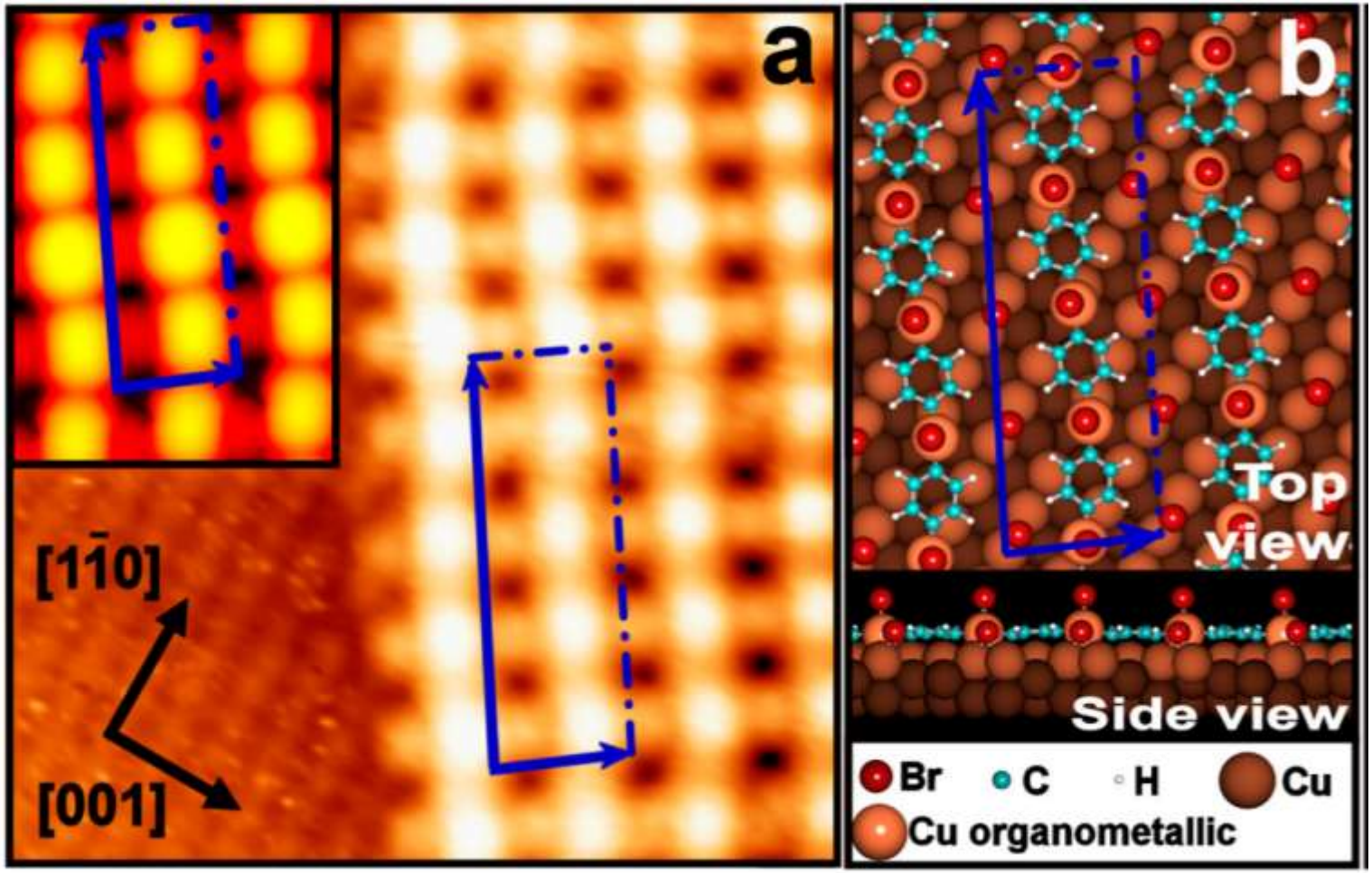
a
b
[1$\bar{1}$0]
[001]
Top view
Side view
Br
C
H
Cu
Cu organometallic

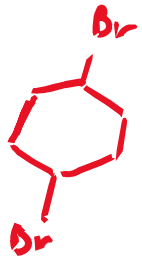

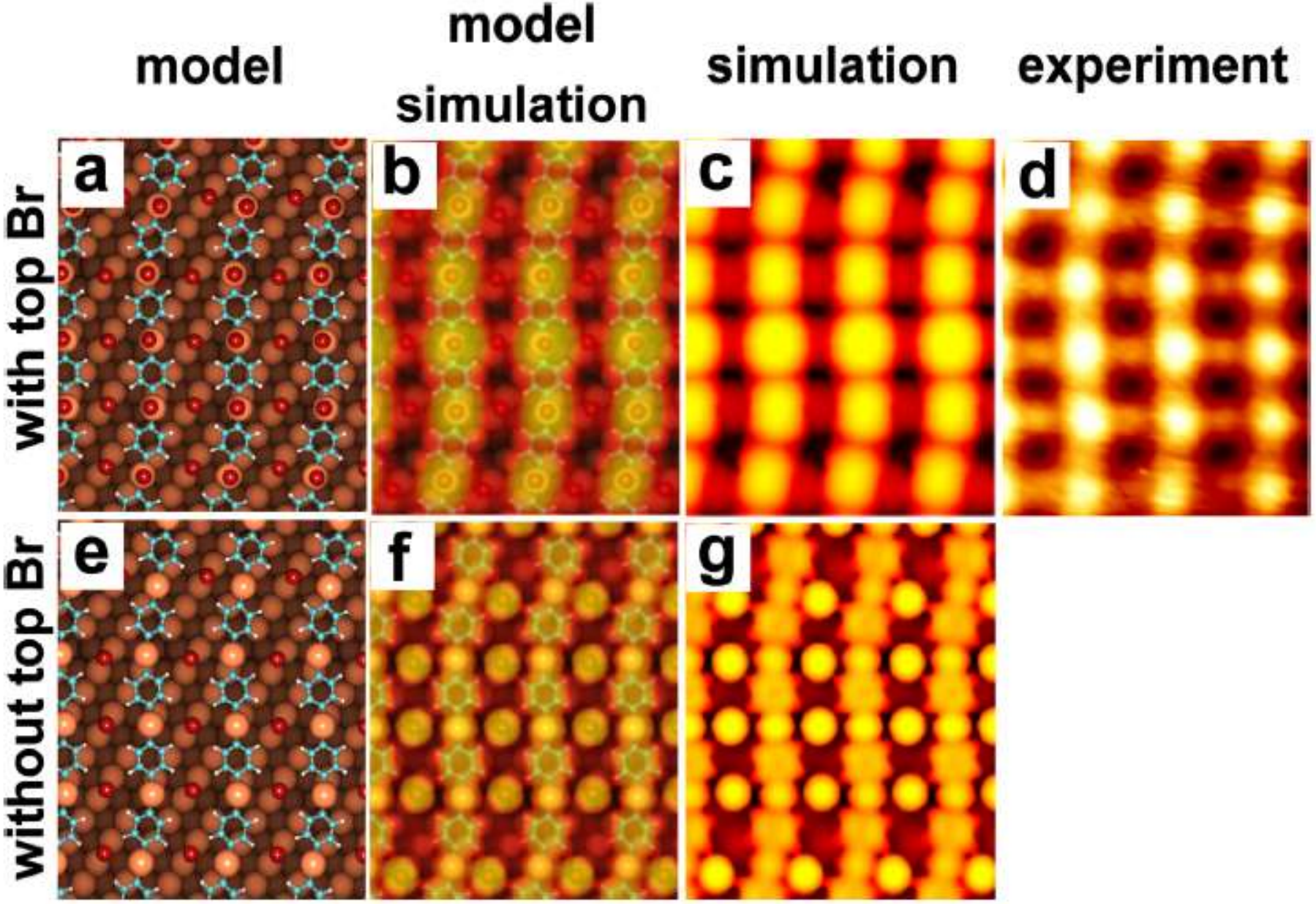
model
model
simulation
simulation
experiment
with top Br
without top Br
a
b
c
d
e
f
g

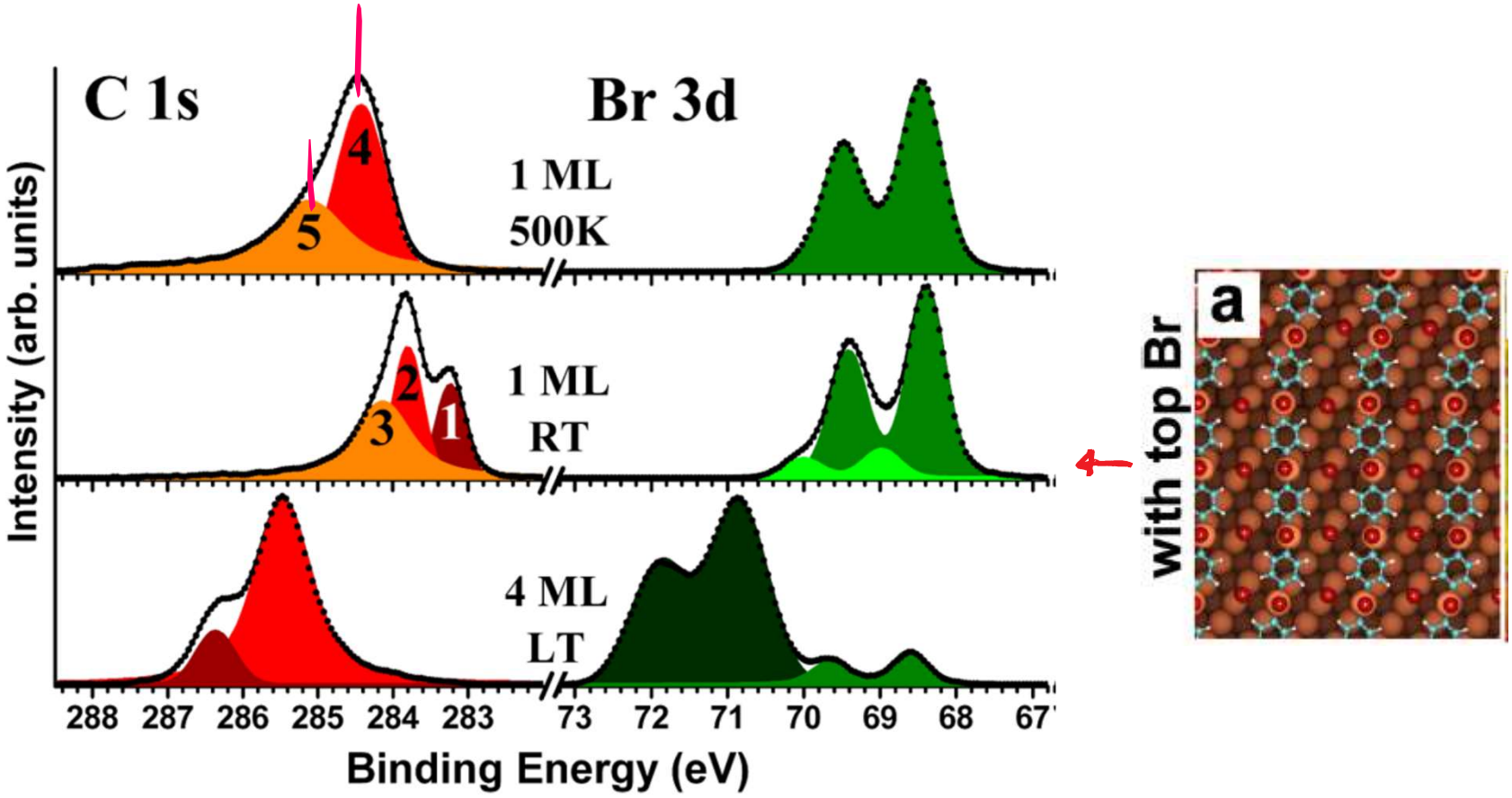
C 1s
Br 3d
1 ML
500K
1 ML
RT
4 ML
LT
5
4
2
3
1
Intensity (arb. units)
288 287 286 285 284 283
73 72 71 70 69 68 67
Binding Energy (eV)
with top Br
a

Annealing a 500 K

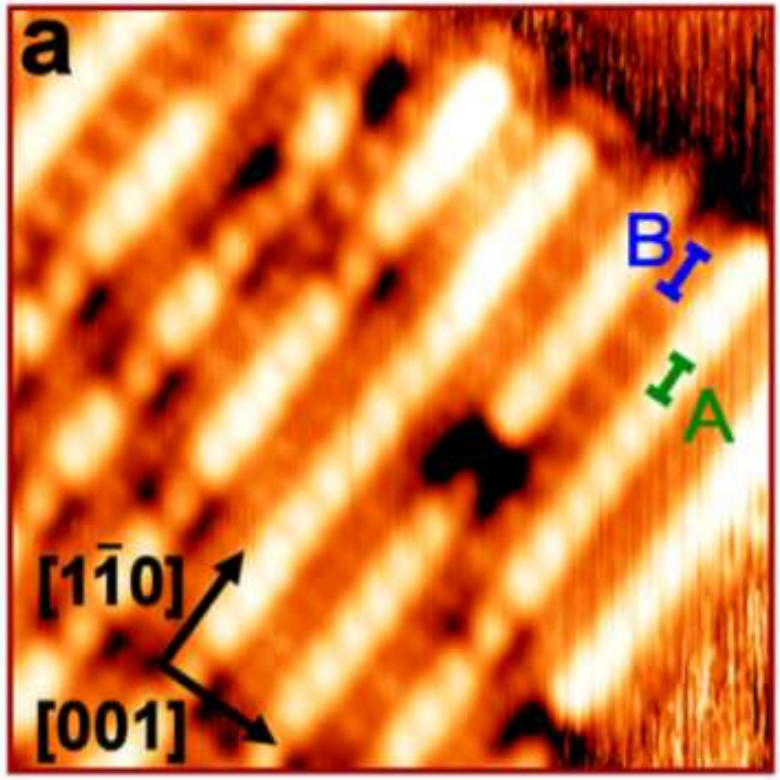

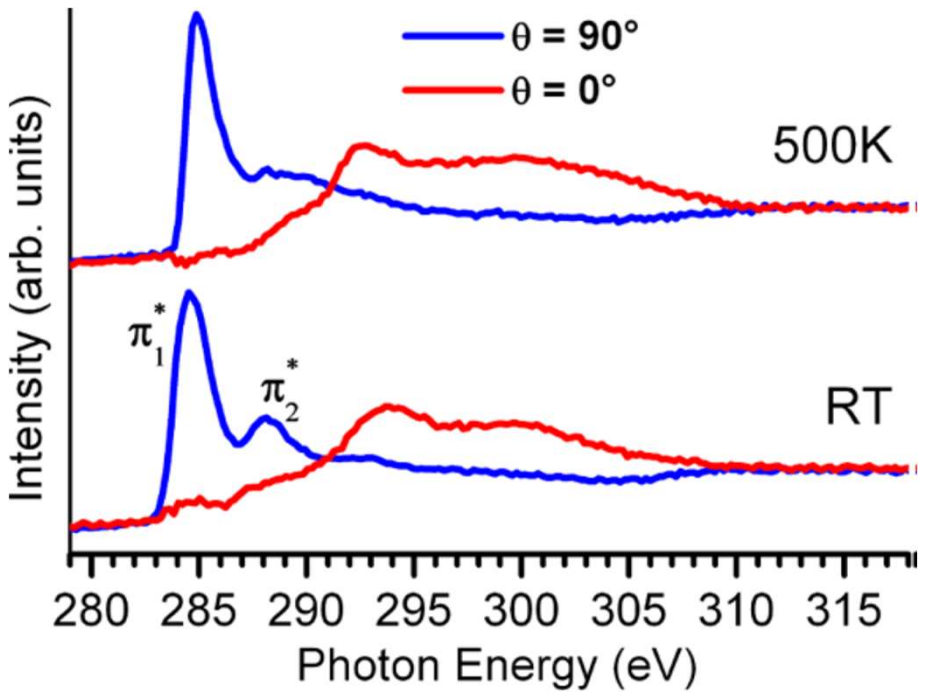

VOL. 7 ▪ NO. 9 ▪ 8190–8198 ▪ 2013 ACSNANO www.acsnano.org

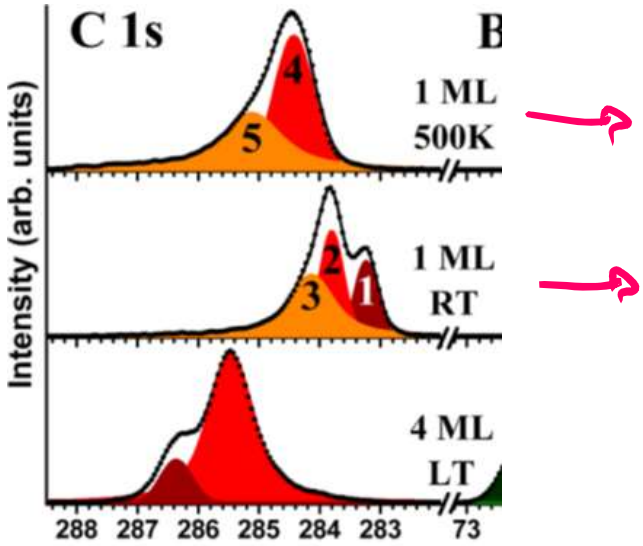

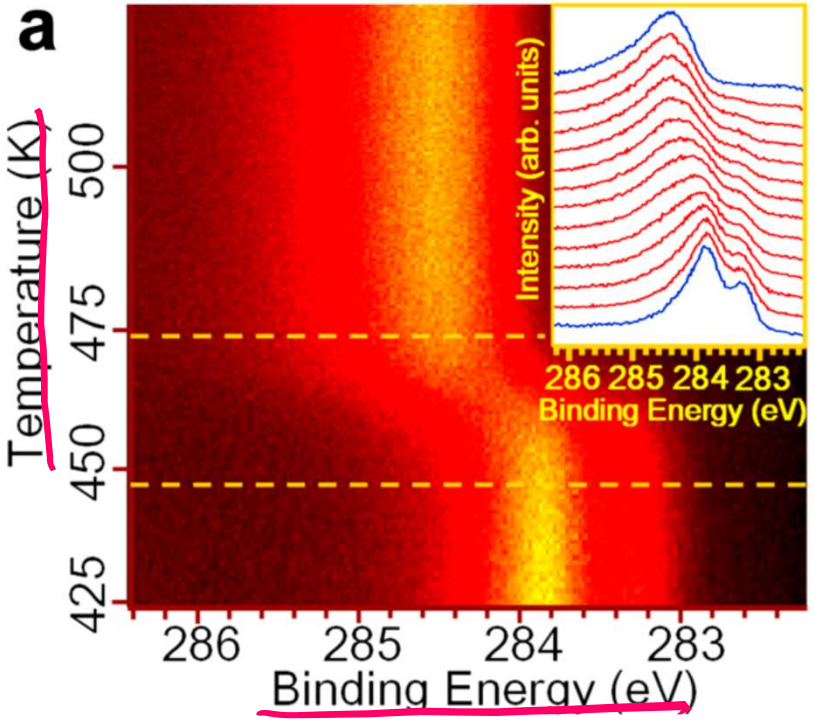

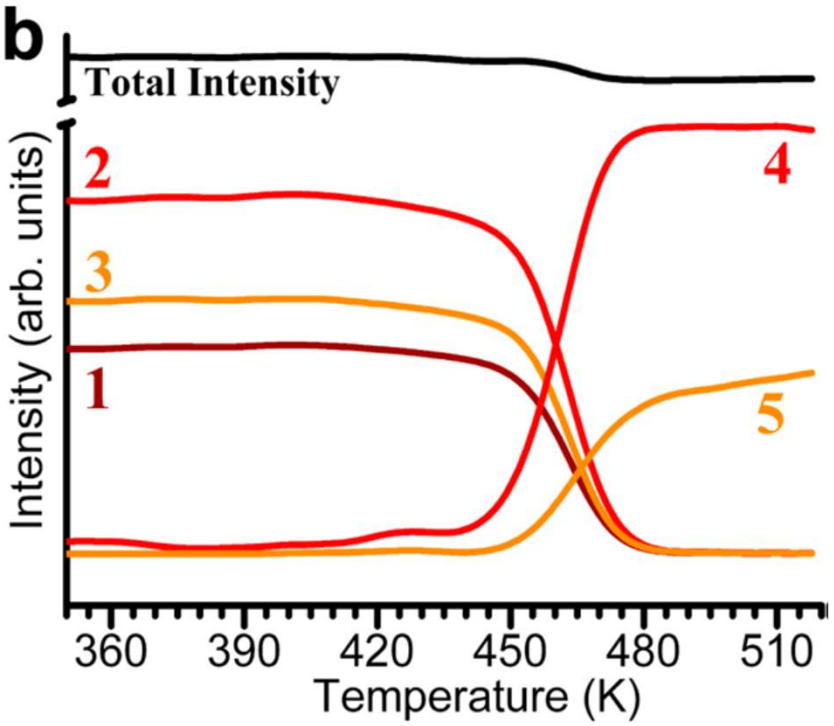

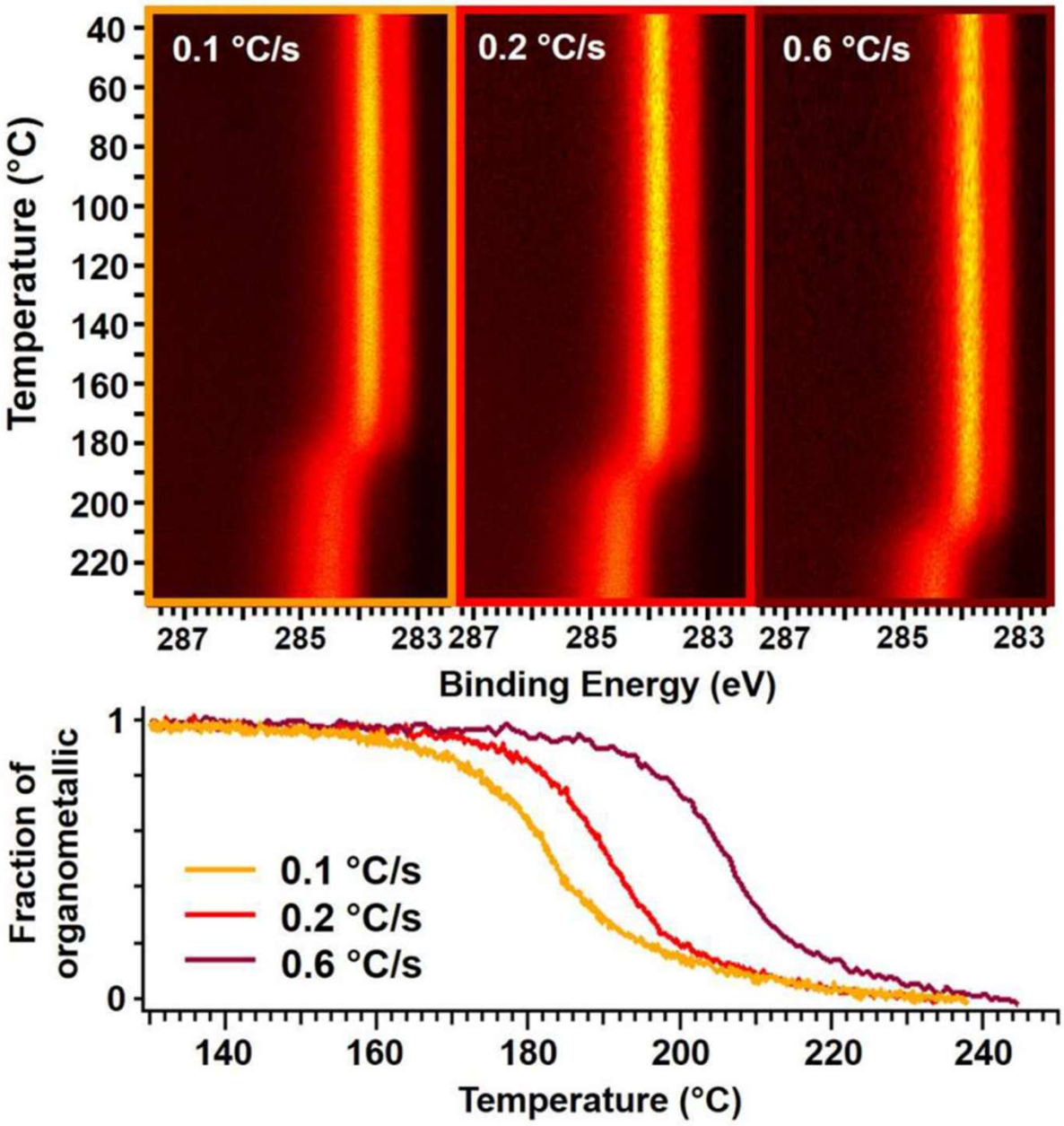
0.1 °C/s
0.2 °C/s
0.6 °C/s
Temperature (°C)
40
60
80
100
120
140
160
180
200
220
287
285
283
Binding Energy (eV)
Fraction of organometallic
1
0
0.1 °C/s
0.2 °C/s
0.6 °C/s
140
160
180
200
220
240
Temperature (°C)

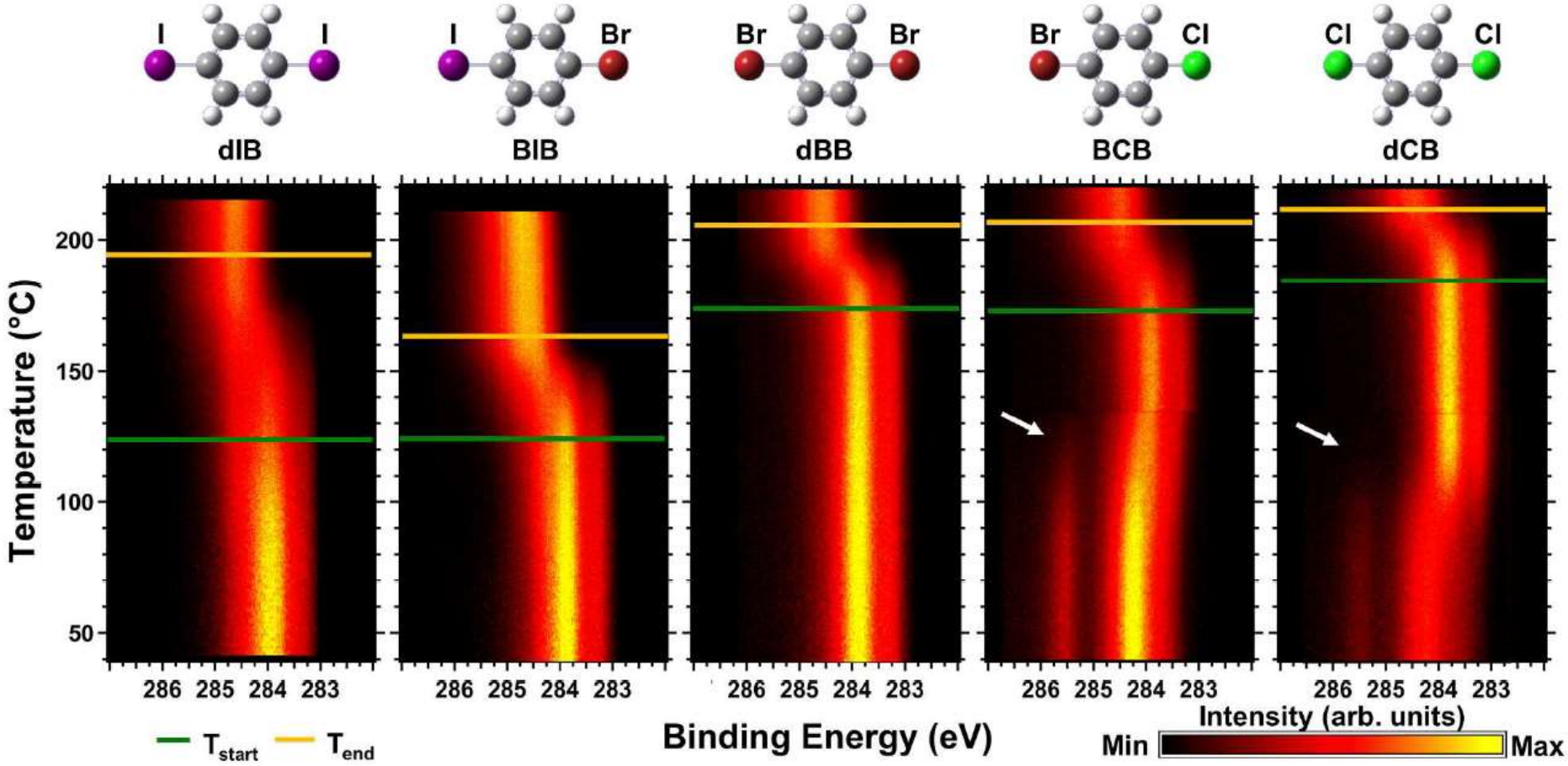
I
I
dIB
I
Br
BIB
Br
Br
dBB
Br
Cl
BCB
Cl
Cl
dCB
Temperature (°C)
200
150
100
50
286 285 284 283
Binding Energy (eV)
T start
T end
Intensity (arb. units)
Min
Max

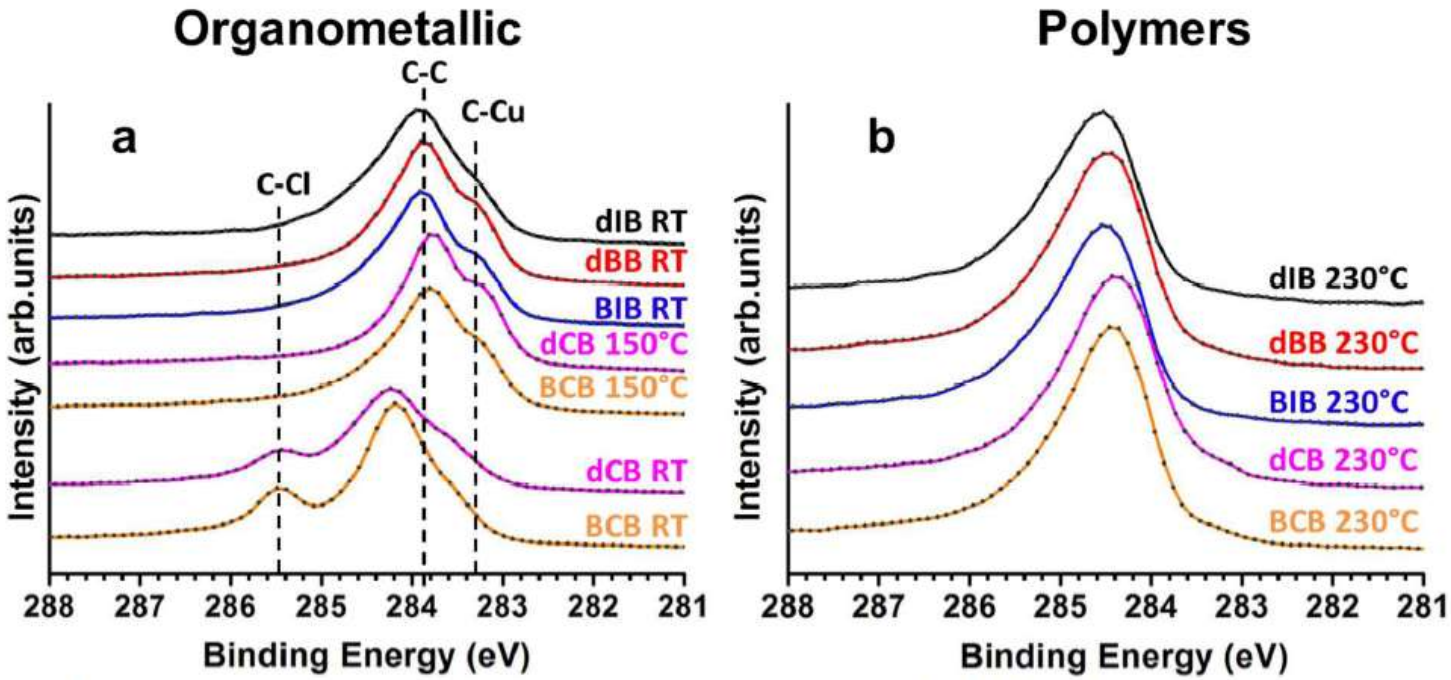

Figure 2. C 1s spectra for a saturated coverage of each precursor on Cu(110) for the organometallic (a) and polymer (b) phases.

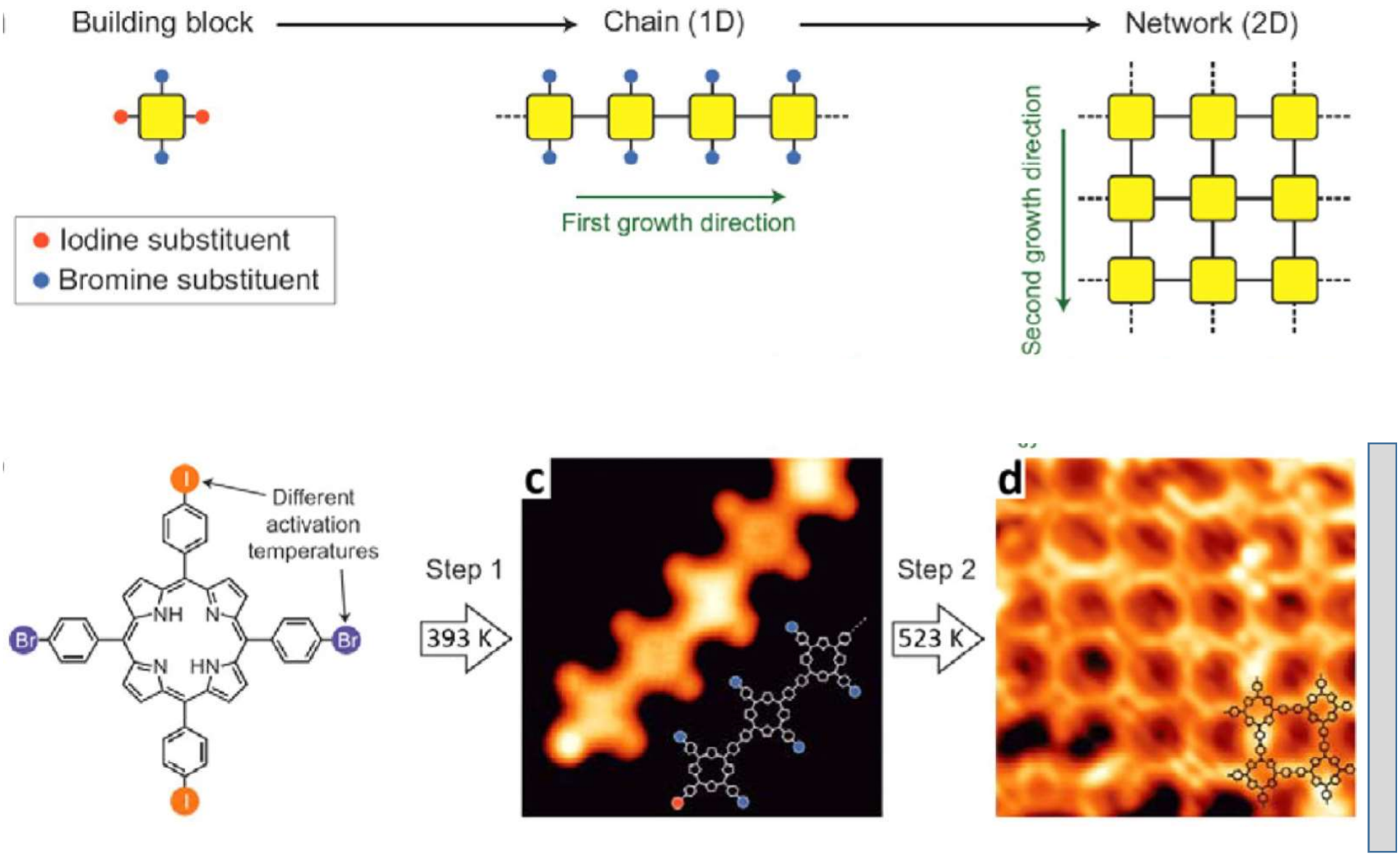
Building block
Chain (1D)
Network (2D)
Iodine substituent
Bromine substituent
First growth direction
Second growth direction
Different activation temperatures
Step 1
393 K
Step 2
523 K
c
d

Boronic condensation

2D Covalent Organic Frameworks

Boronic COF

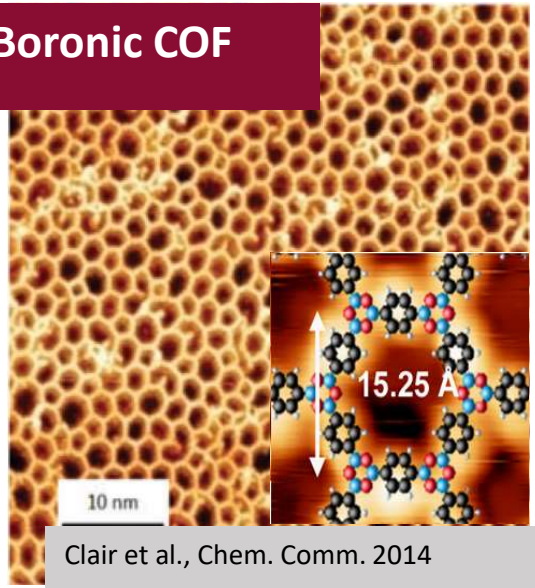

Clair et al., Chem. Comm. 2014

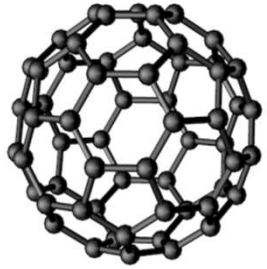

fullerene

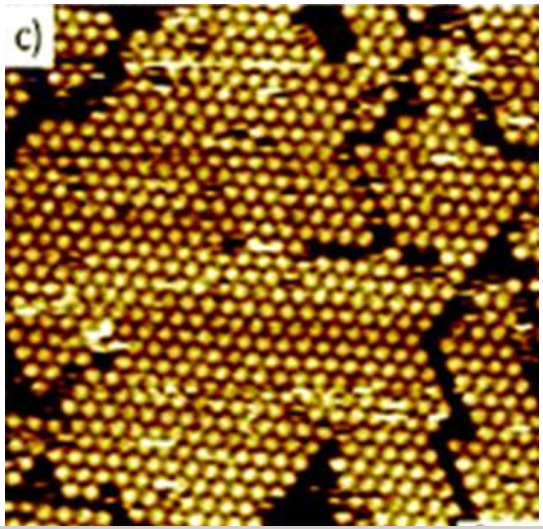

Plas et al., Chem. Comm. 2016

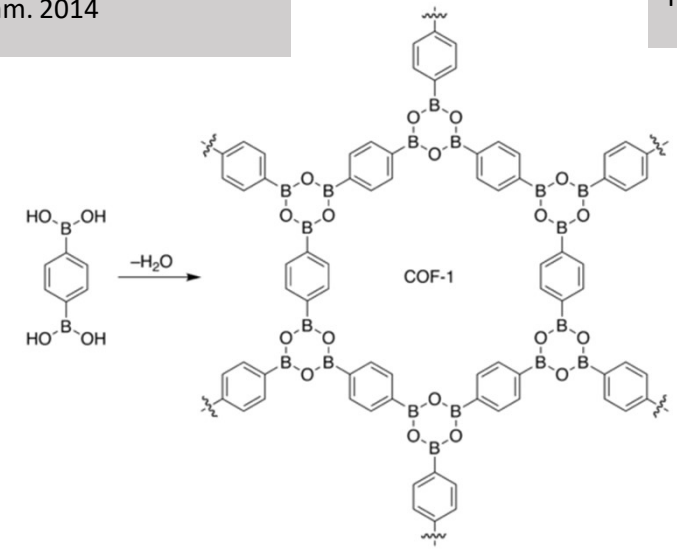

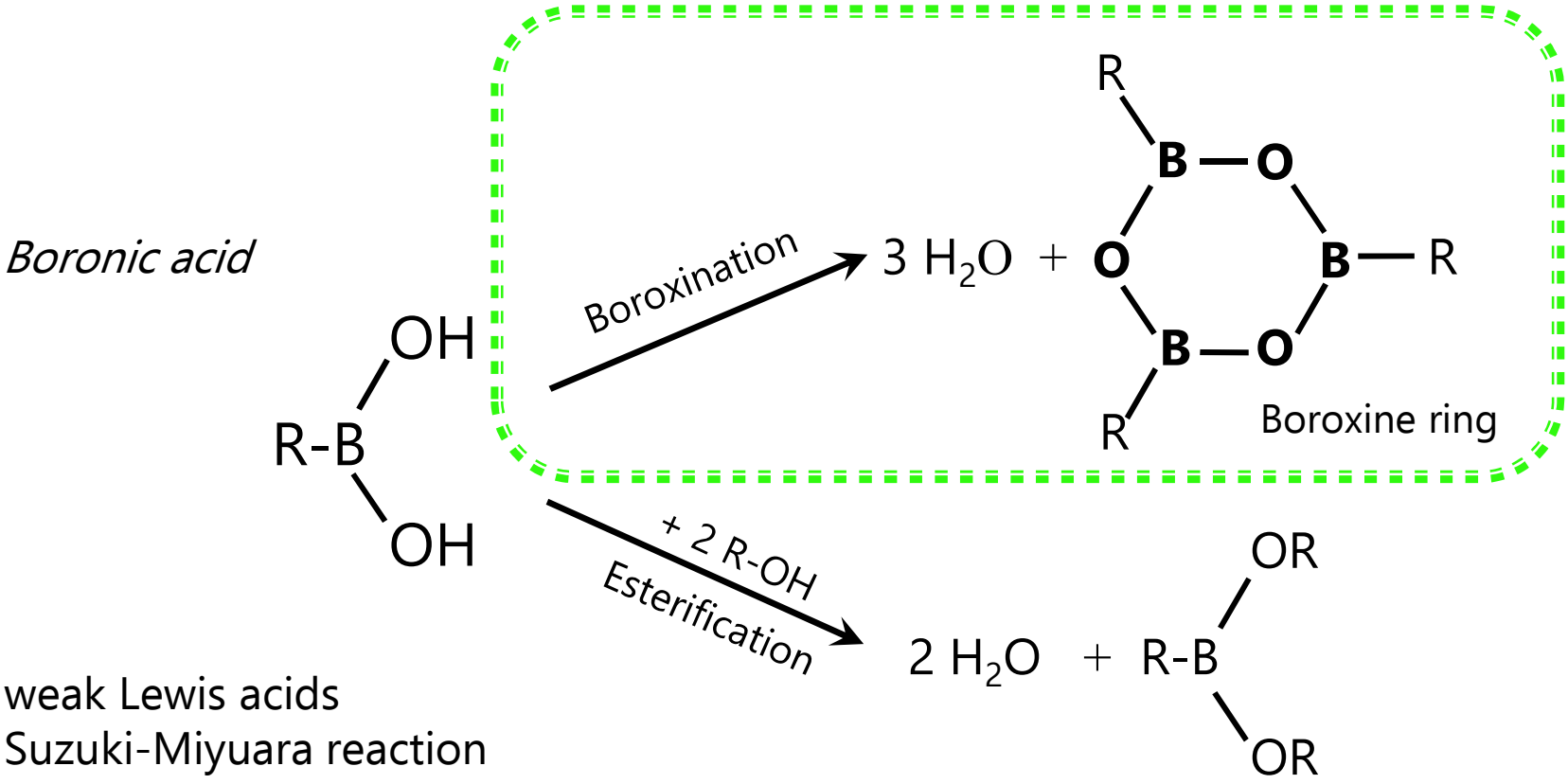

weak Lewis acids
Suzuki-Miyuara reaction
detection of sugars
molecular imprinting

1

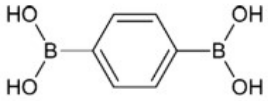

2

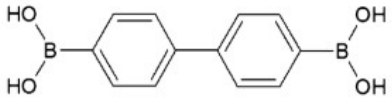

3

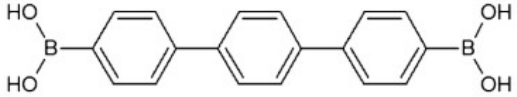

4

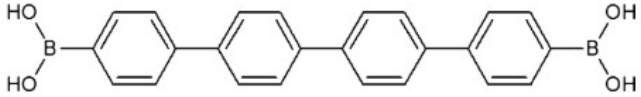

5

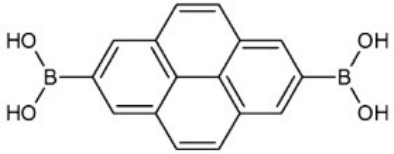

Evaporabile in UHV

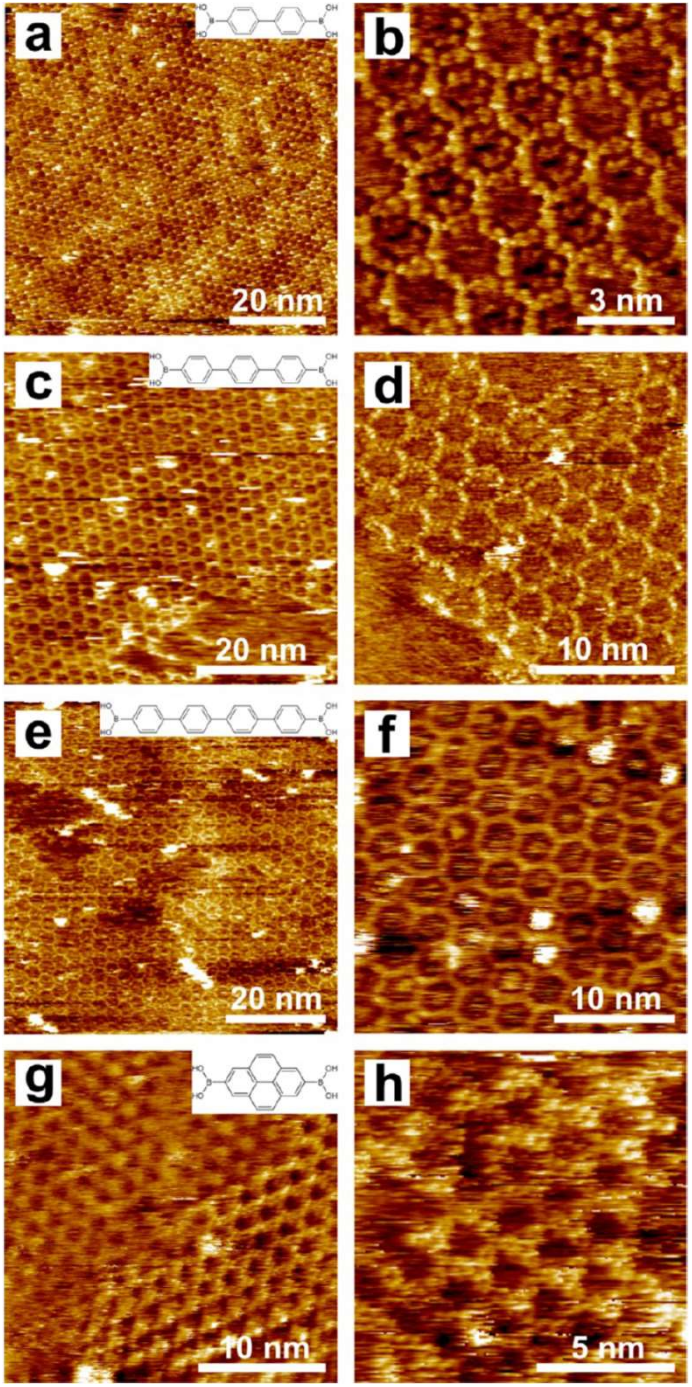

Sequenza condensazione boronica - Ullmann

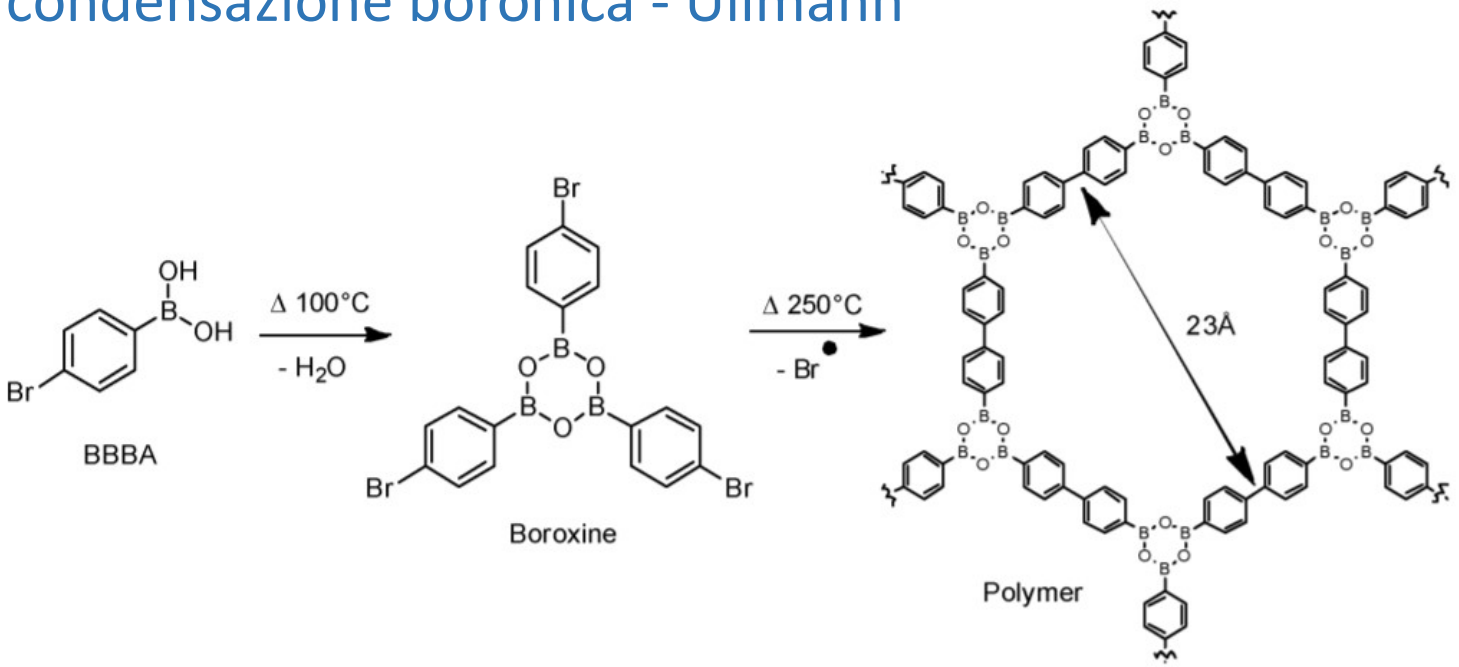

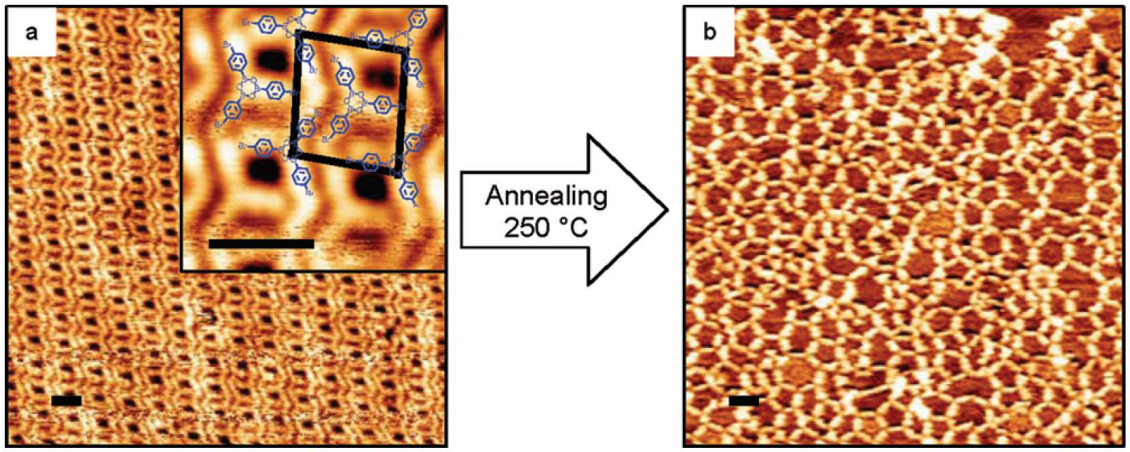

J. Phys. Chem. C 2012, 116, 4819–4823

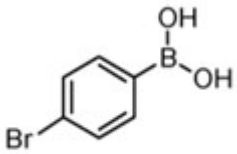

BBBA

Ts=250°C

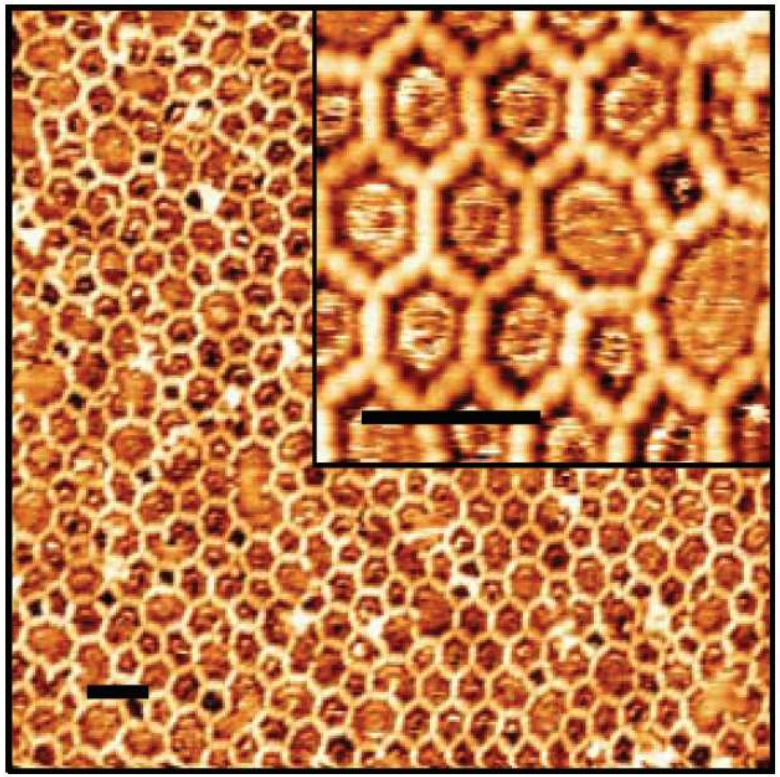

J. Phys. Chem. C 2012, 116, 4819–4823

Boroxine macromolecules

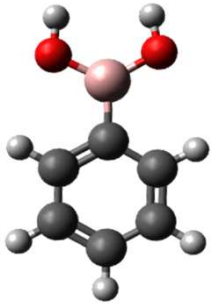

Phenylboronic acid
on Au(111)

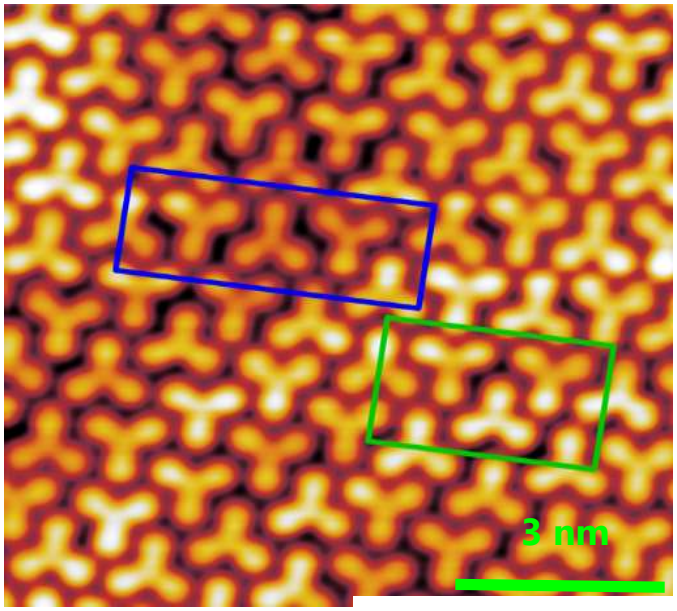

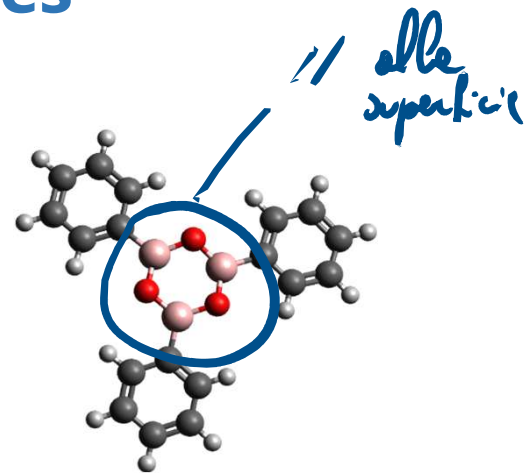

On surface synthesis
Triphenylboroxine

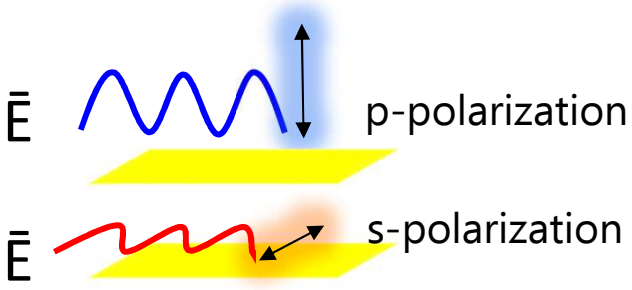

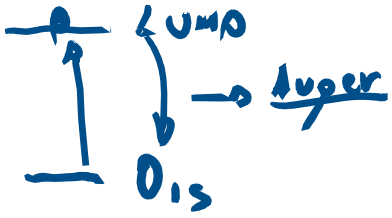

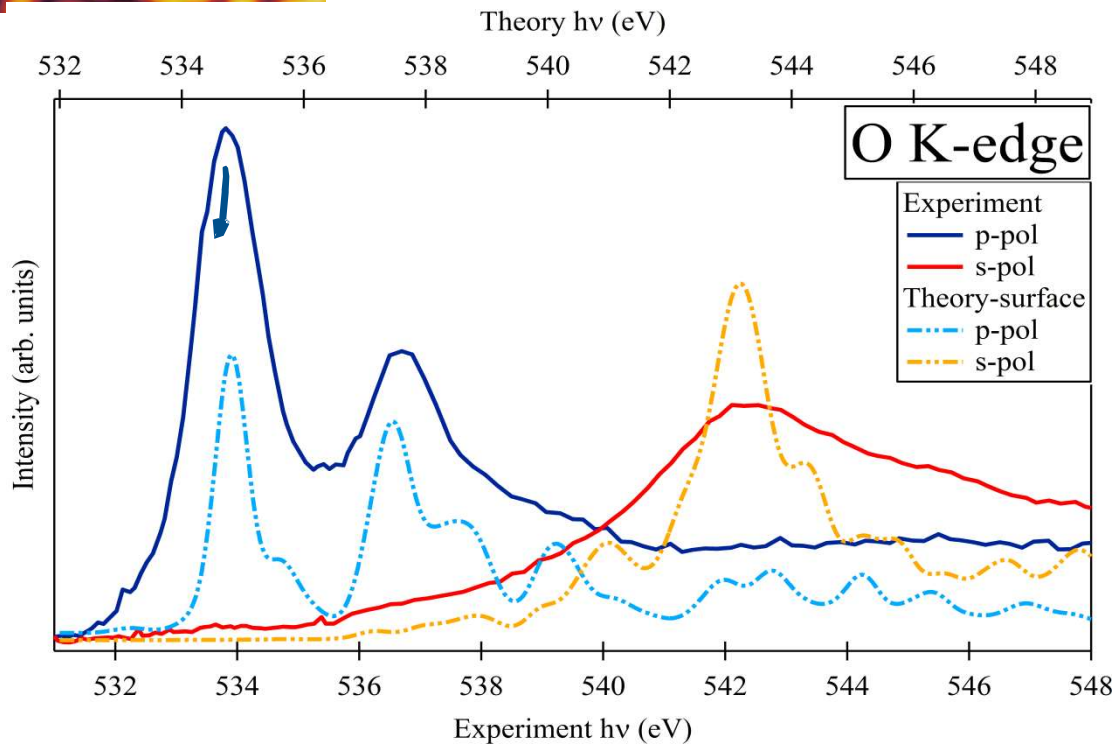

Chem. Sci., 2017, 8, 3789-3798

$T < -50°C$ → deposizione multilayer del precursore

Il rapporto $\frac{O_{1s}}{B_{1s}}$ sia maggiore nel multilayer

$h\nu$ la probabilità di fotoemissione da un certo livello (O_{1s}, B_{1s} ...) dipende dalla cross section ($\sigma_{O_{1s}}$, $\sigma_{B_{1s}}$)

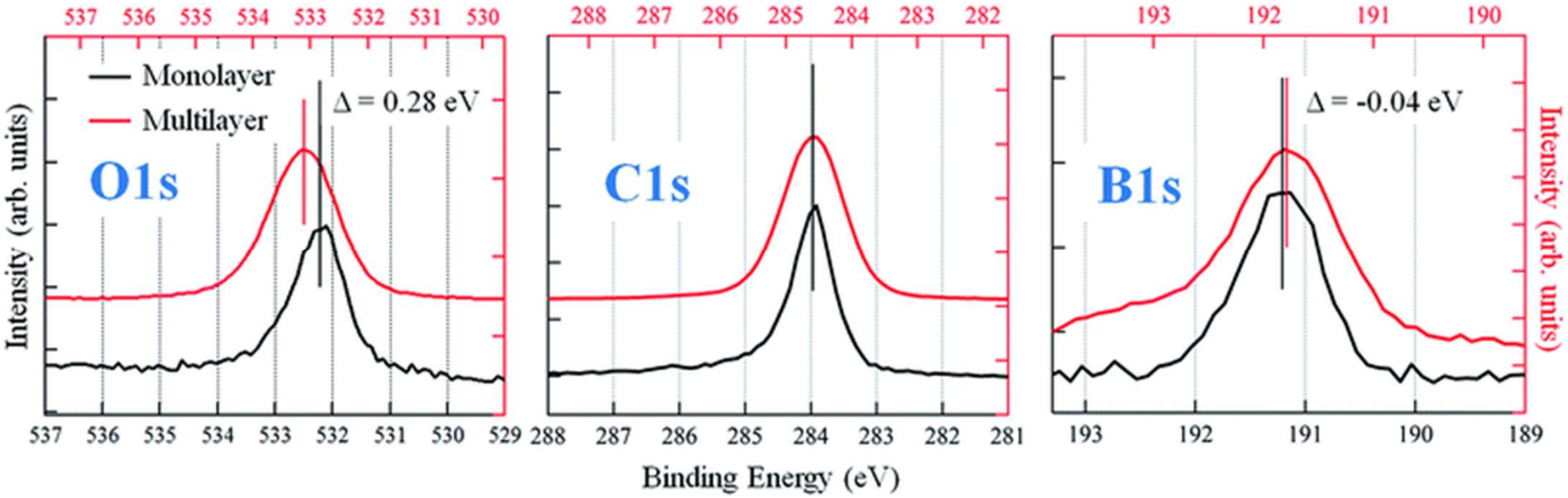

Chem. Sci., 2017, 8, 3789-3798

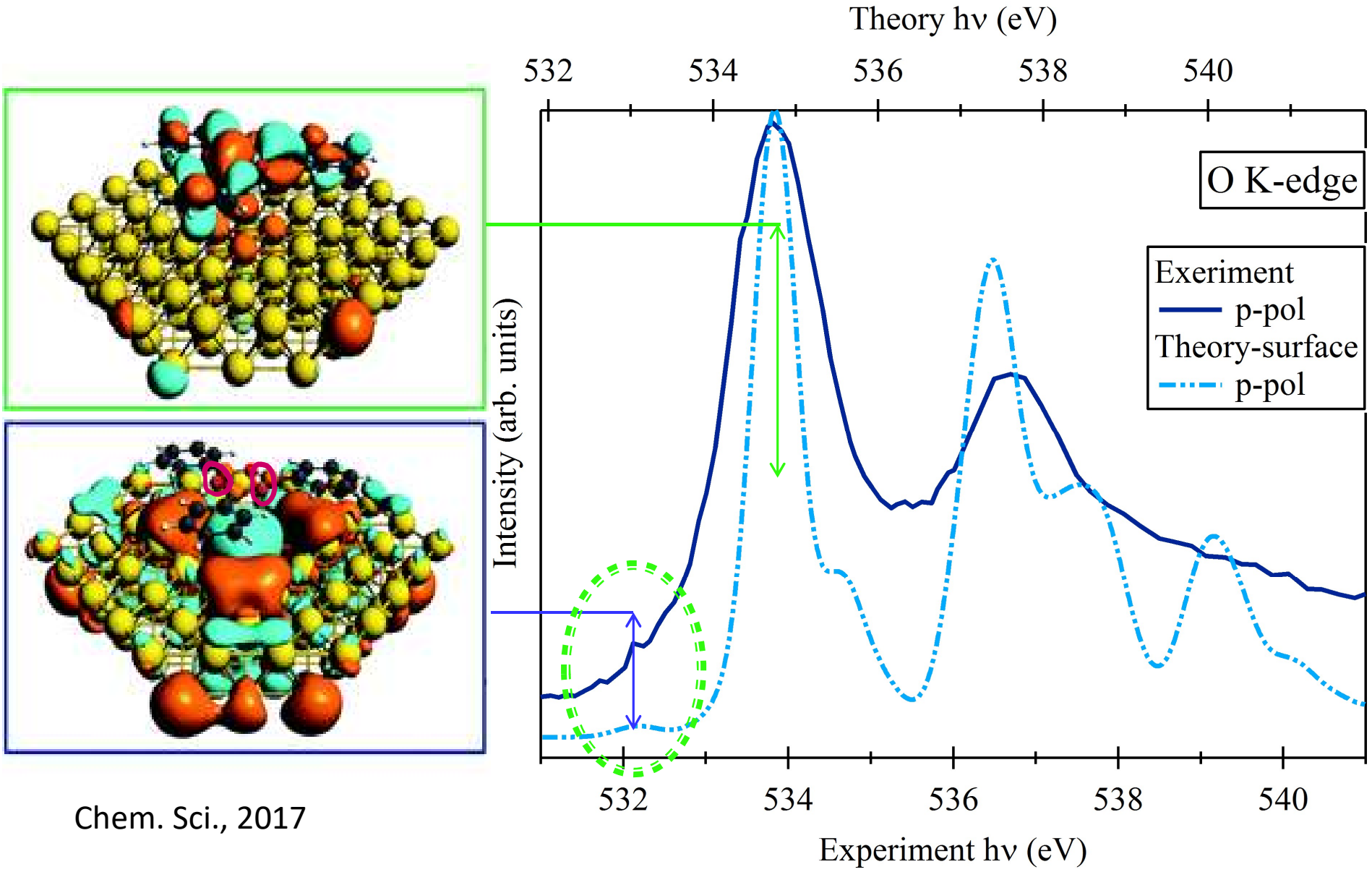

Chem. Sci., 2017

O k-edge RESPES: IMO promotes ultra-fast charge delocalization

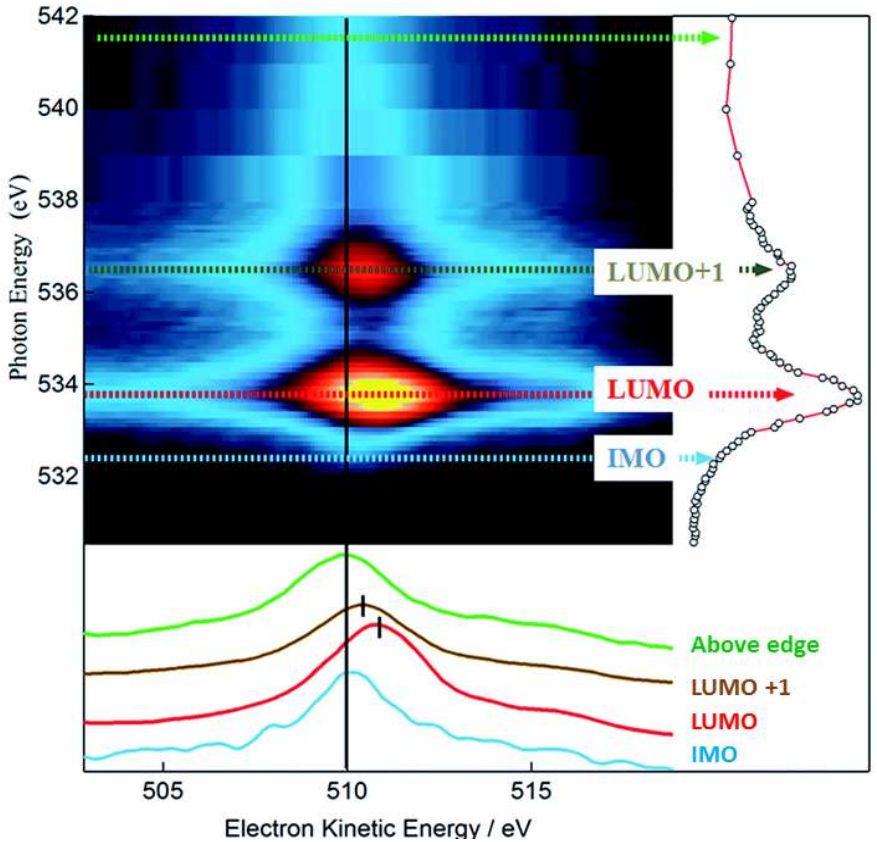

platforms for

ultrafast charge transfer

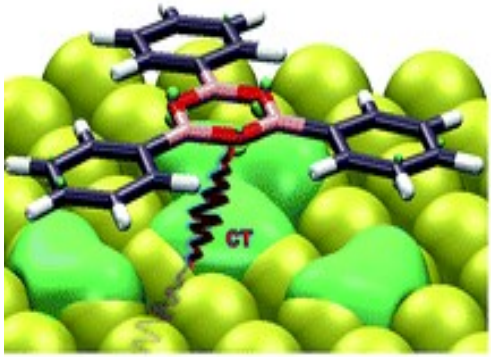

Toffoli et al., Chem. Sci., 2017, **8**, 3789-3798

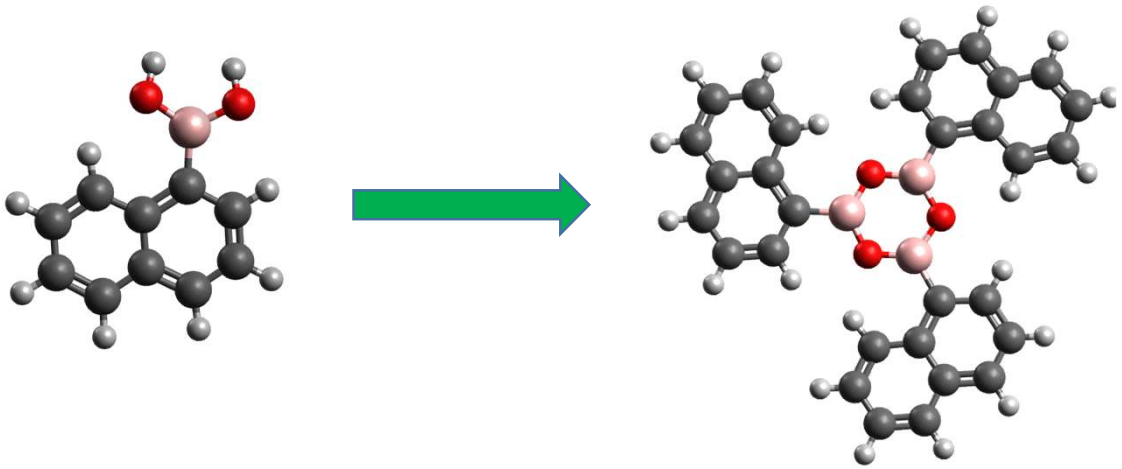

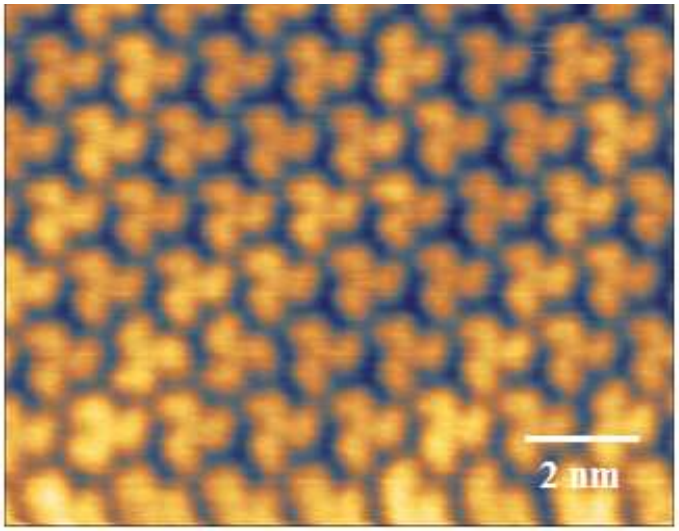
2 nm

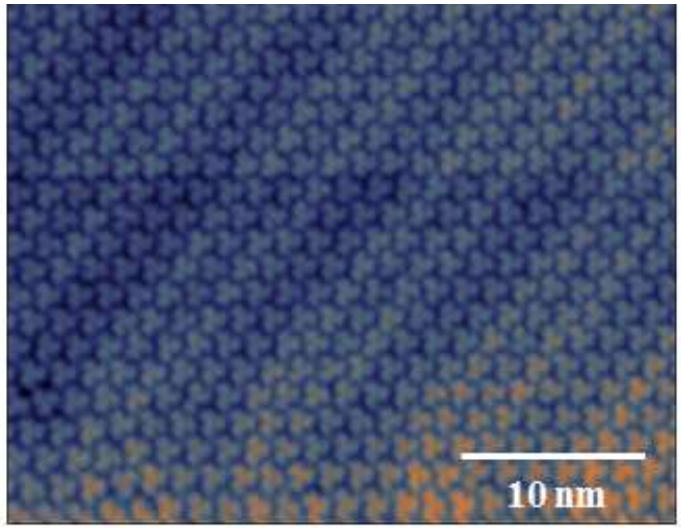
10 nm

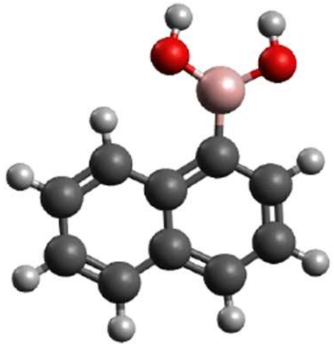

NBA su Au(111)

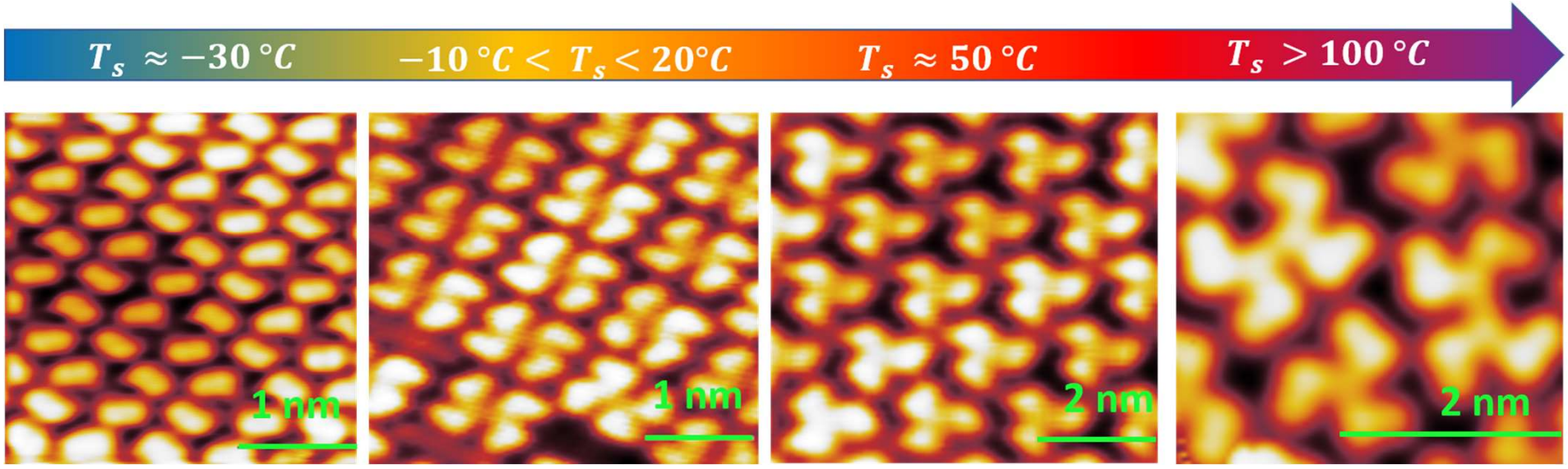

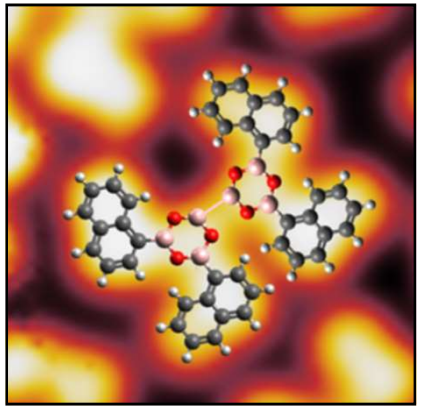

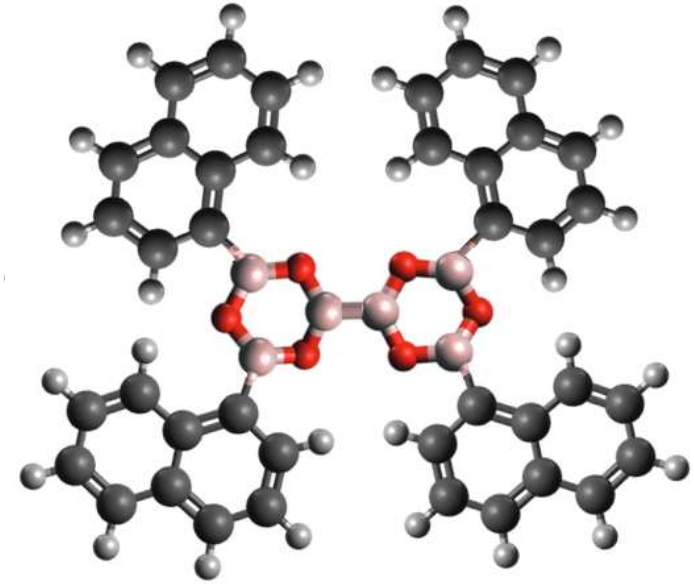

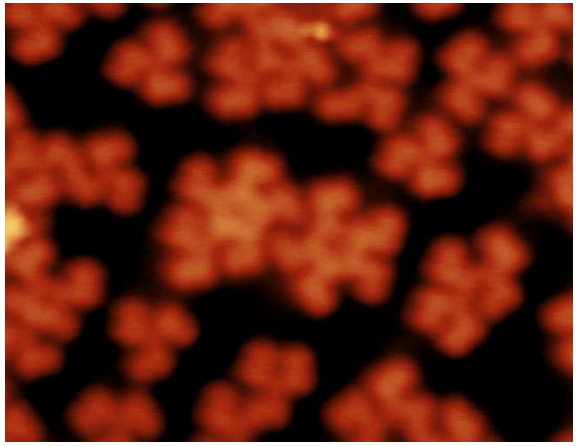

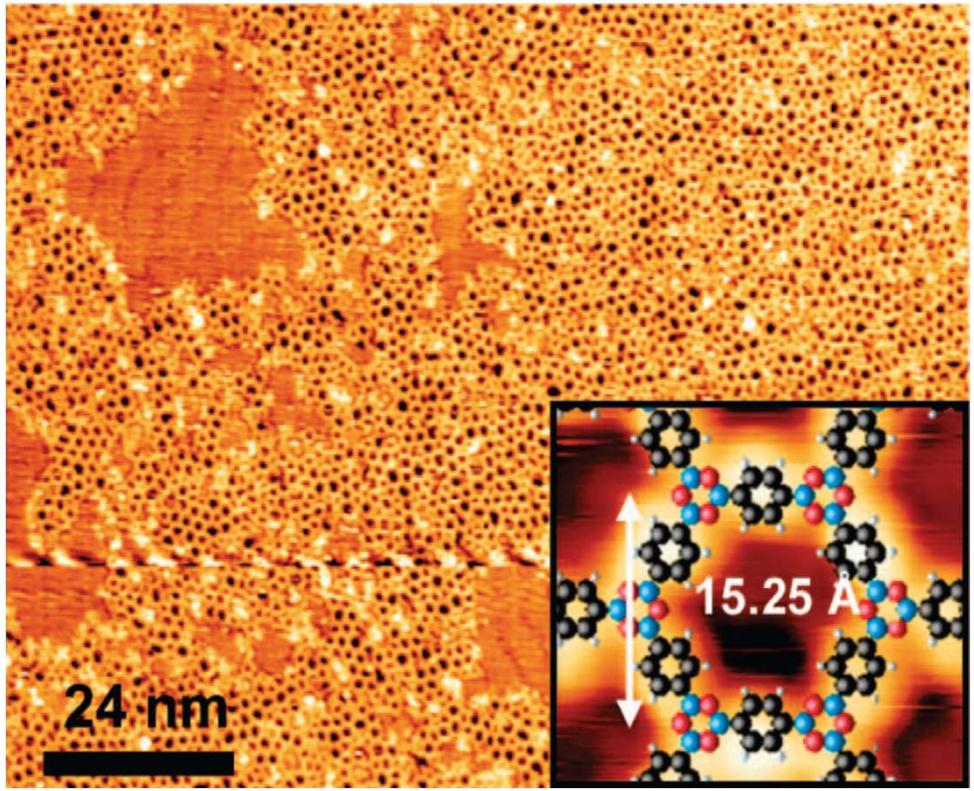

T. Faury et al., J. Phys. Chem. C 2012, 116, 4819−4823

DFT calculations:
Boroxine rings break the aromaticity of phenyl rings

R. Wang, X. Zhang, S. Wang, G. Fu, J. Wang,
Phys.Chem.Chem.Phys.,2016,18,1258

Framework di borossine

THDB
Tetra**h**ydroxy**di**b**o**ron

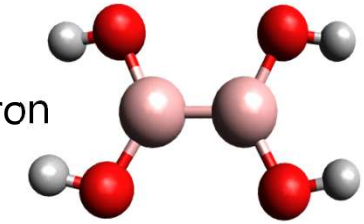

B
O
H

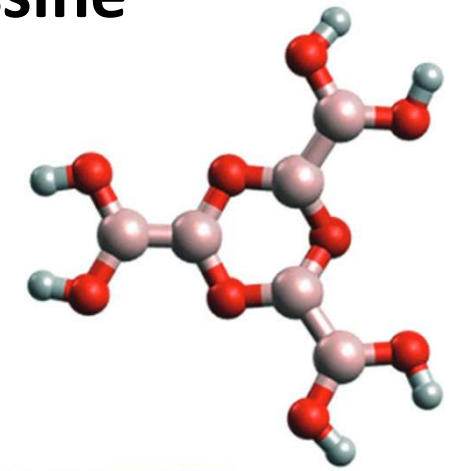

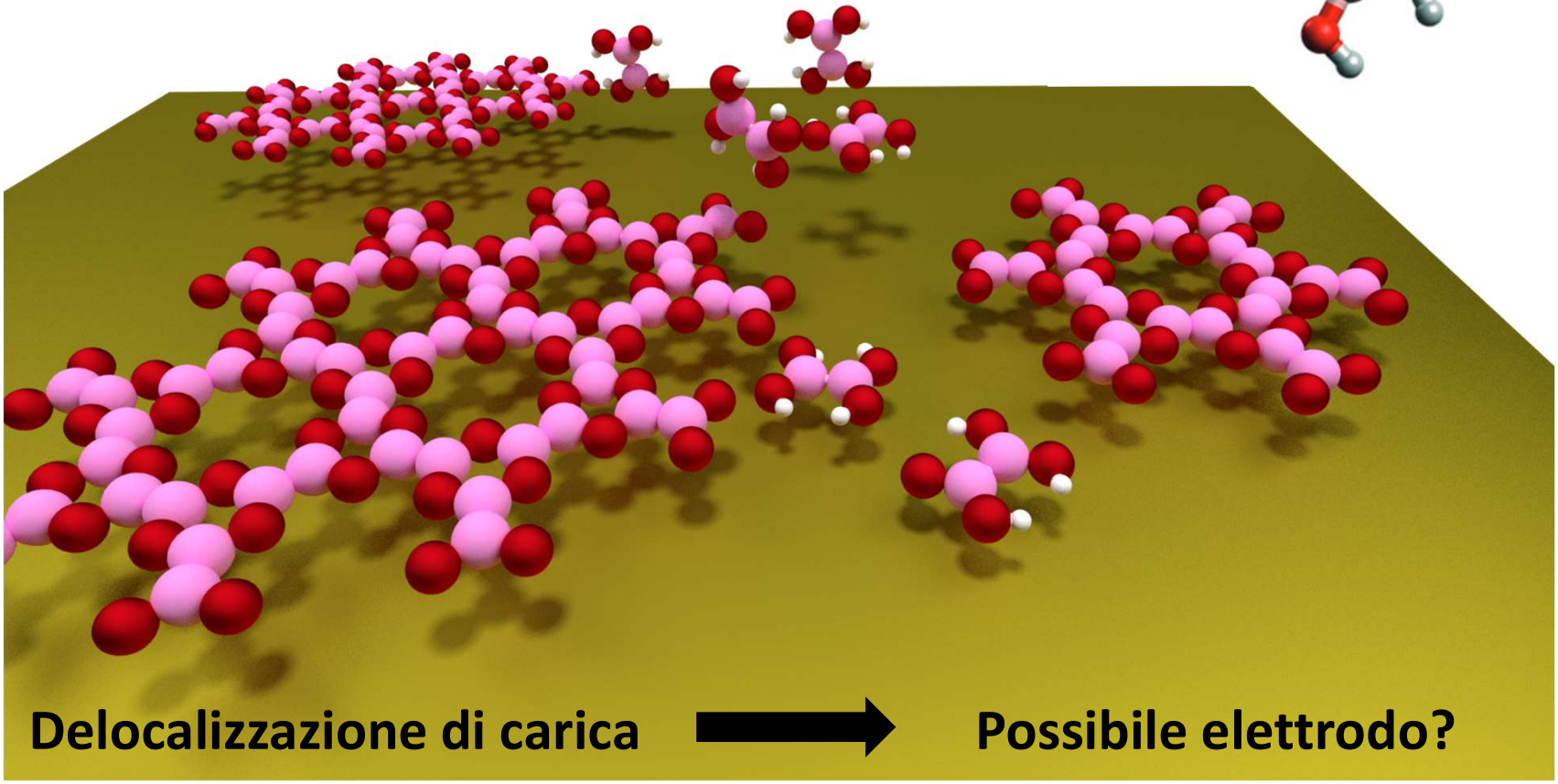

Chem. Commun., 2018

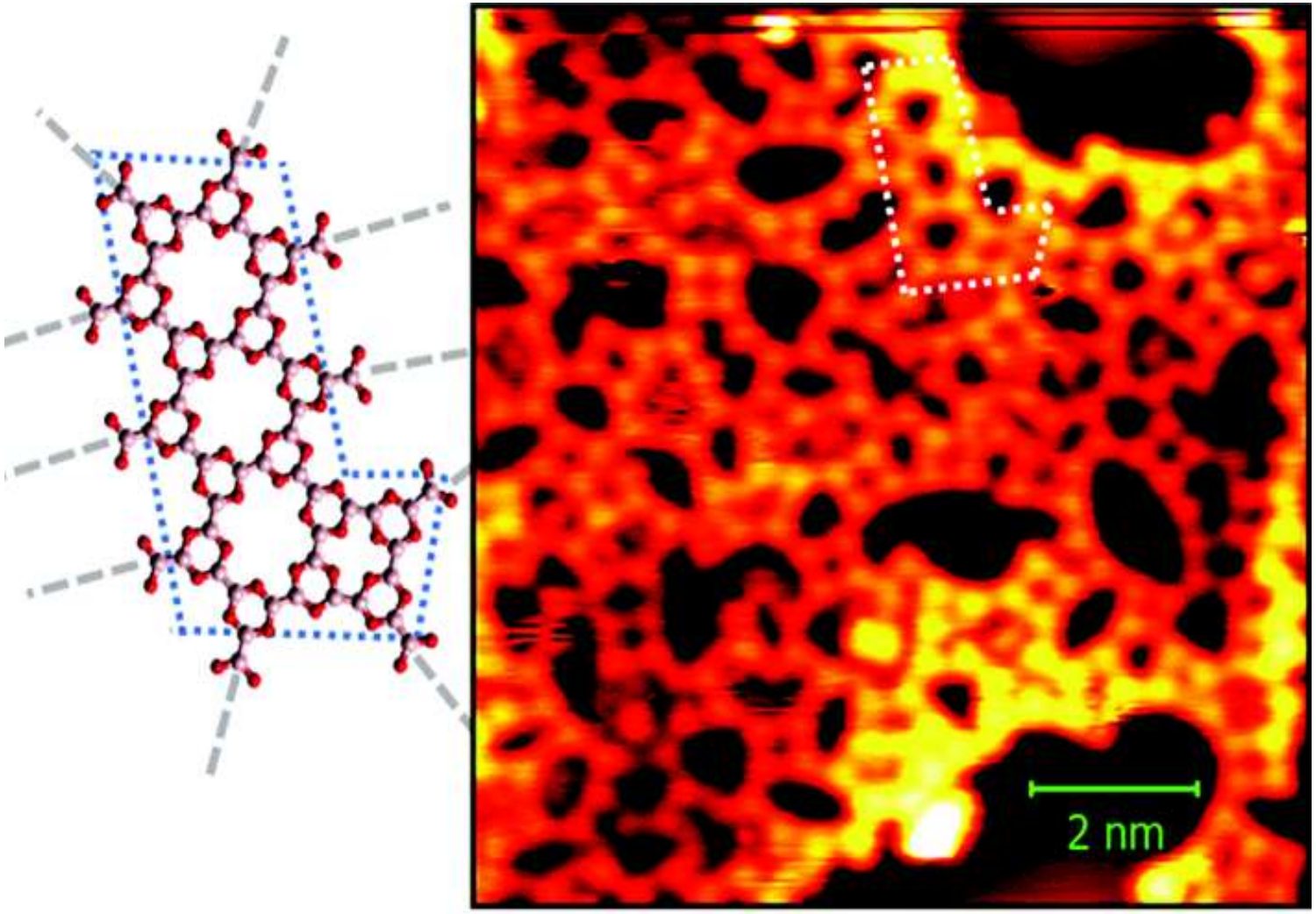

vitreous morphology

Proliferation of defects

Chem. Commun., 2018

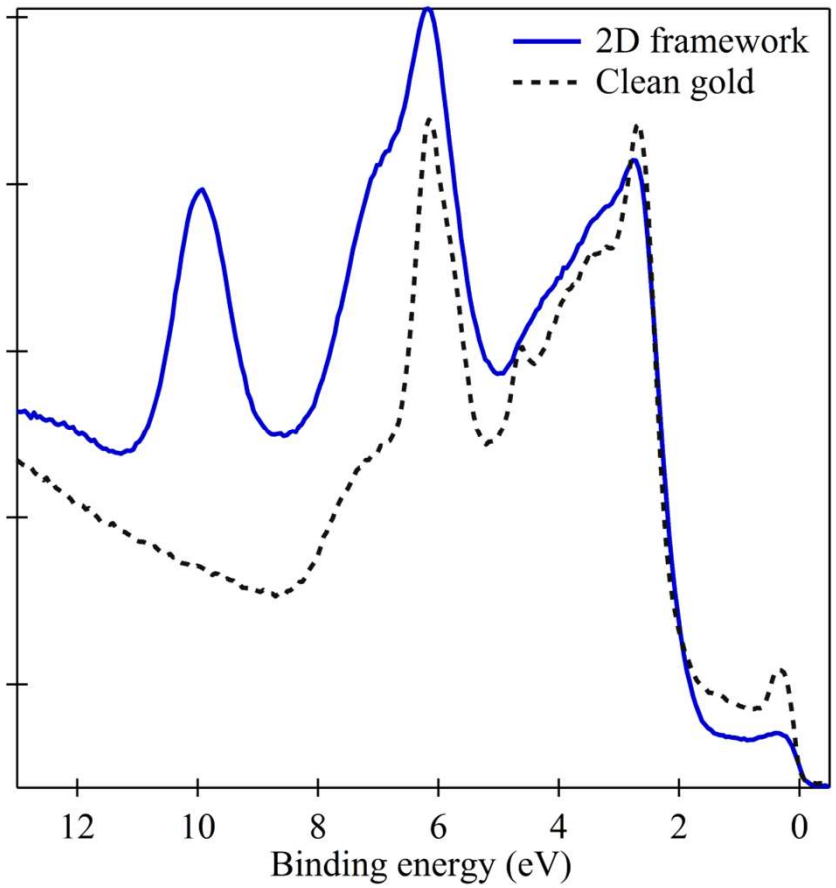

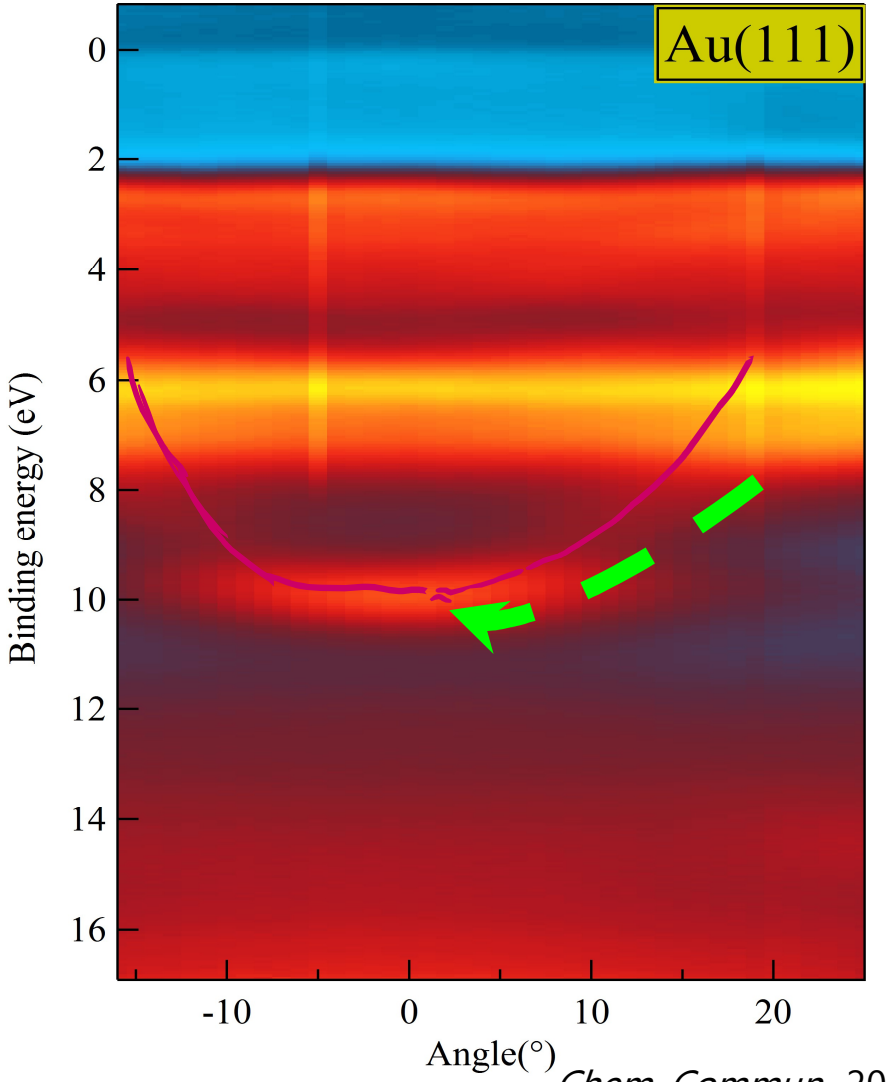

Chem. Commun., 2018

Band dispersion at room temperature – electron delocalization

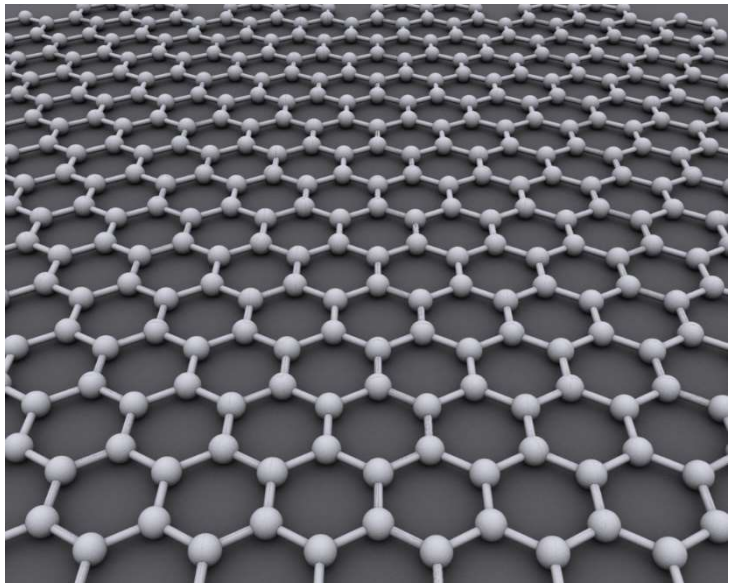

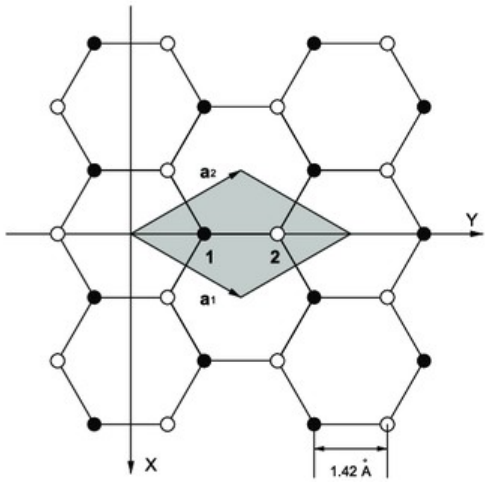
a2
a1
1
2
Y
X
1.42 Å

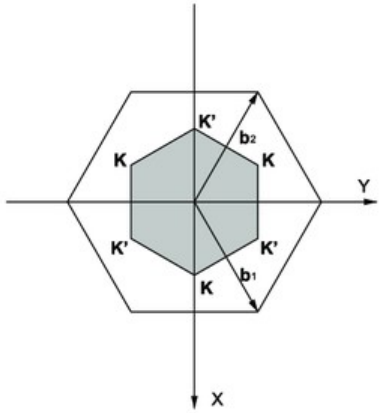
K'
b2
K
K
Y
K'
K'
K
b1
X

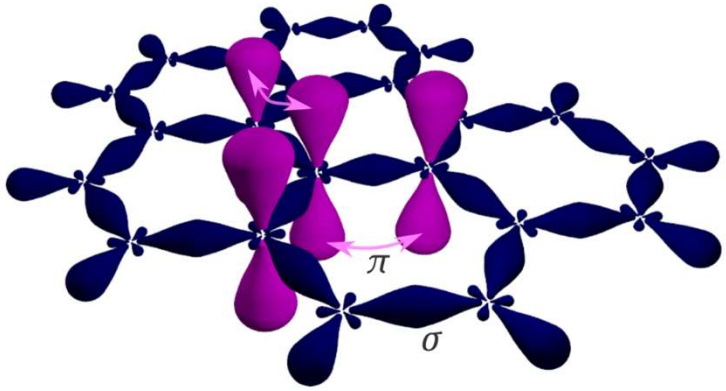
π
σ

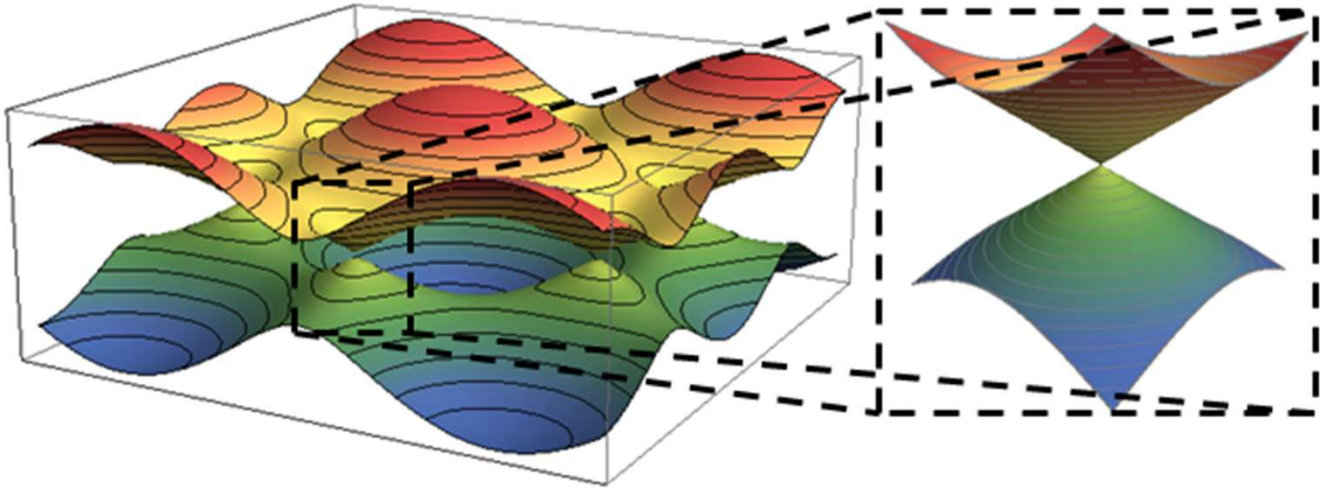

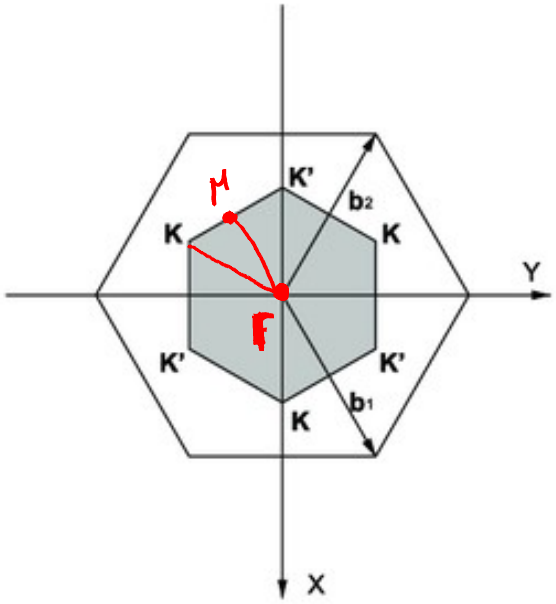
M
K'
b2
K
K
Y
Γ
K'
K'
b1
K
X

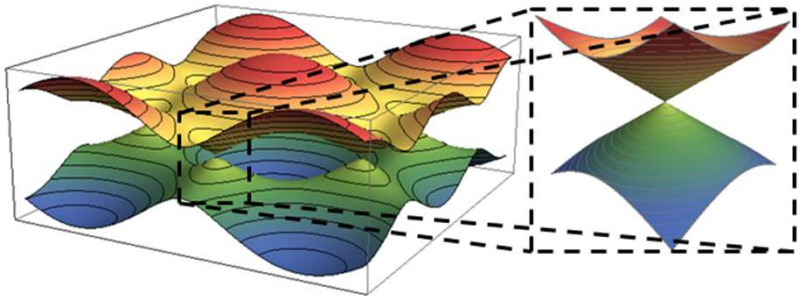

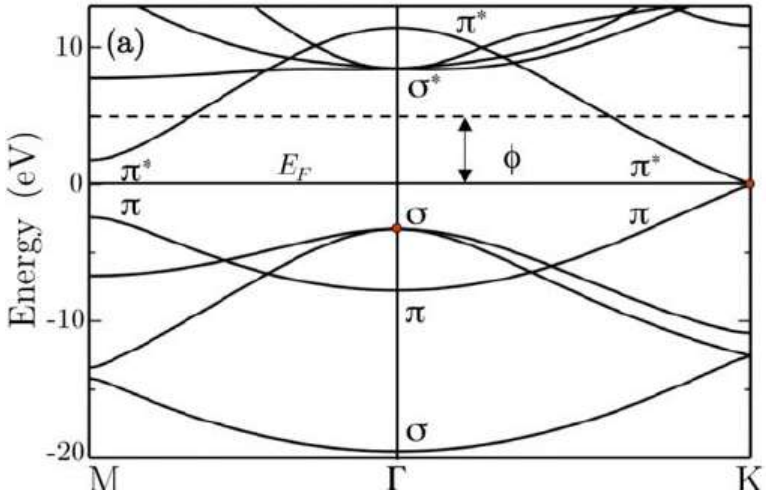
(a)
10
0
-10
-20
Energy (eV)
π*
σ*
ϕ
π*
π*
E_F
π
σ
π
π
σ
M
Γ
K

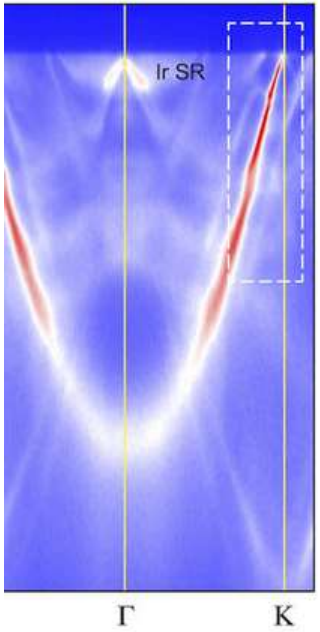

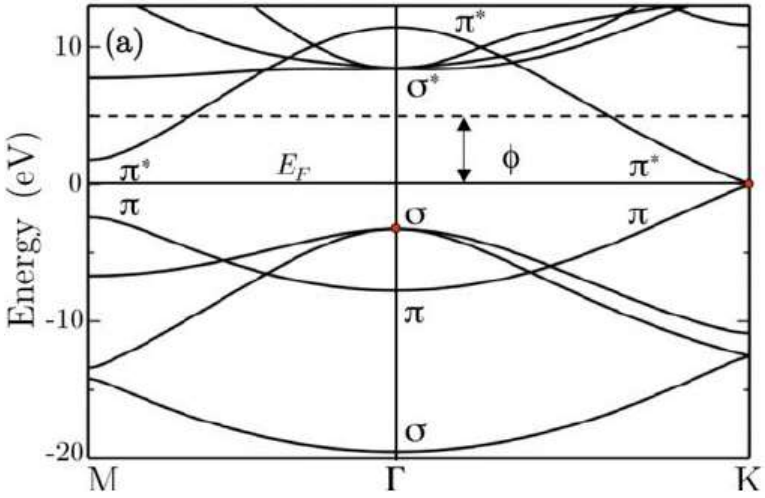

•Journal of Physics Condensed Matter 2015 27(30)

Sintesi di grafene

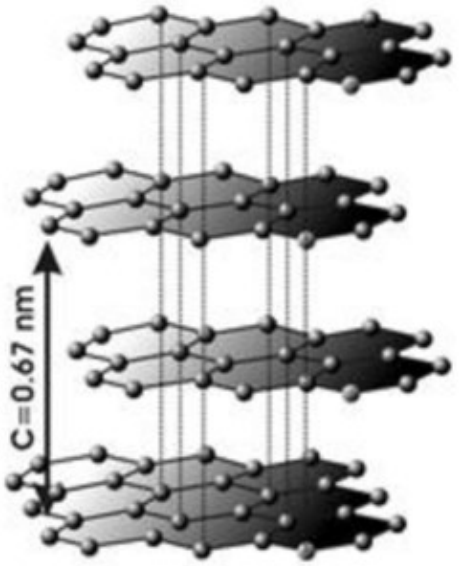

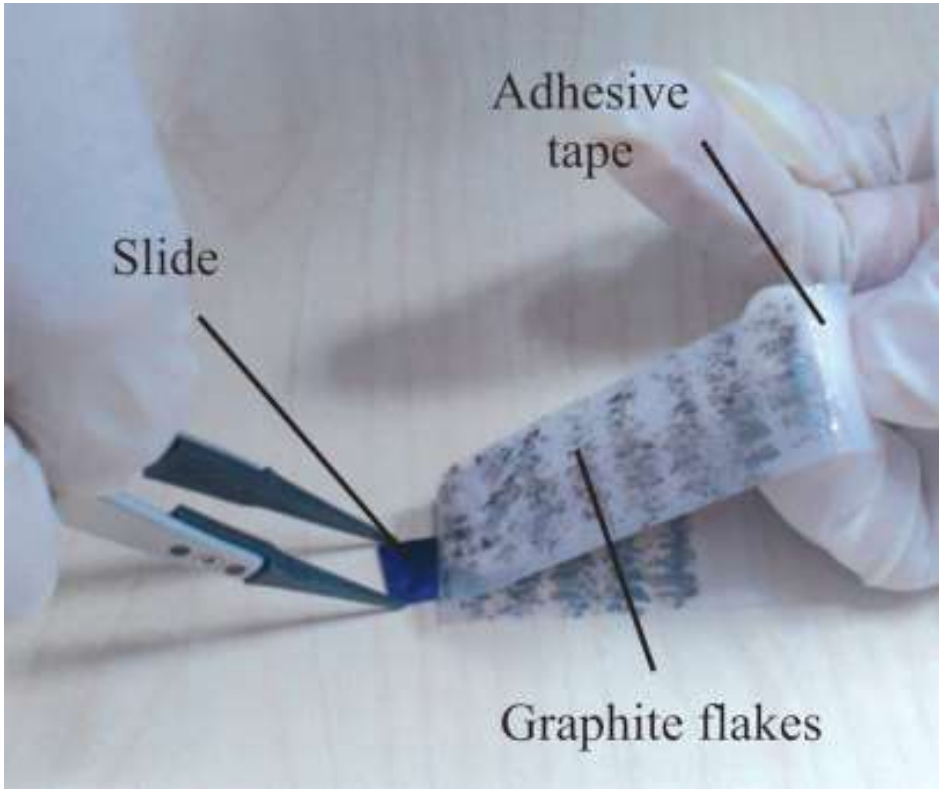
Adhesive
tape
Slide
Graphite flakes


Andre Geim

Chemical Vapour Deposition

Cu (111), 1000 °C

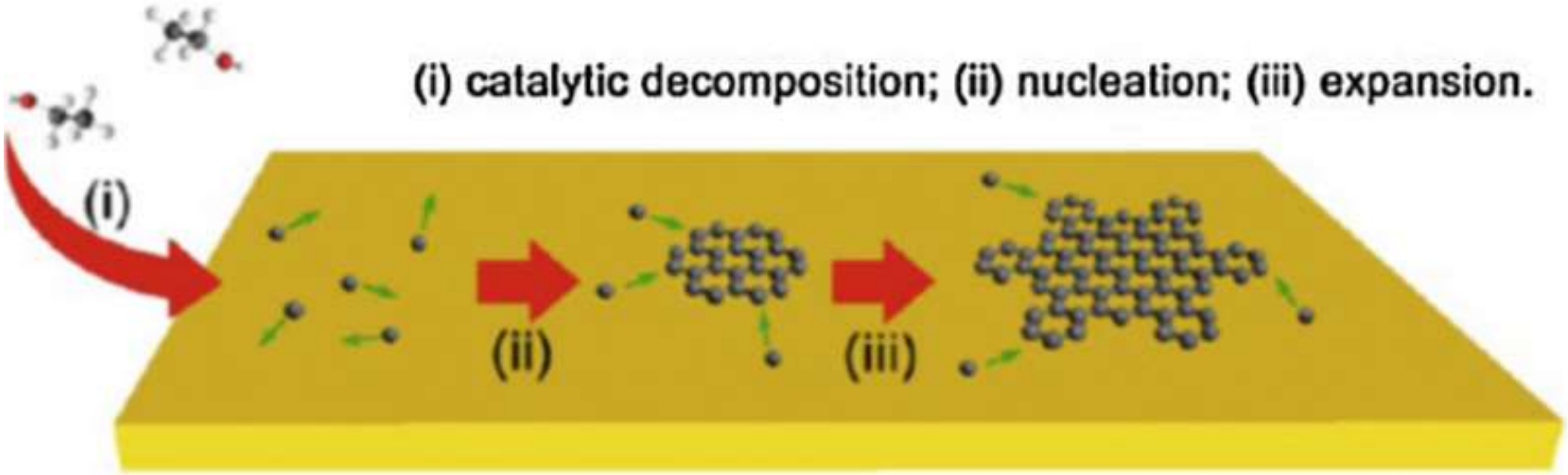

X. Chen et al./Synthetic Metals 210 (2015) 95–108

Ni(111)

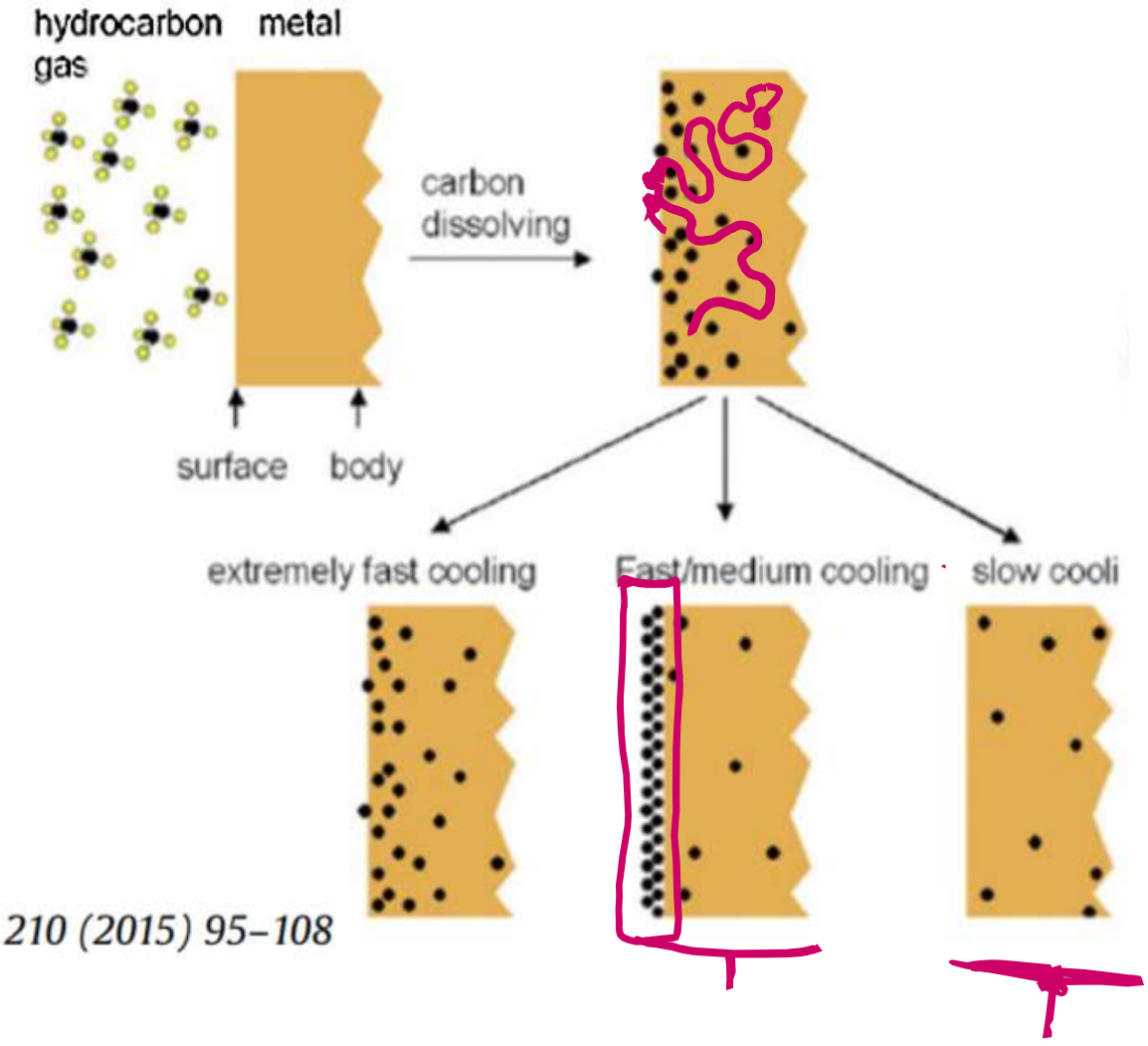

X. Chen et al./Synthetic Metals 210 (2015) 95–108

Table 1 Carbon solubilities (atom%) in different transition metals at 1000 °C according to ref. 17

Metal	Carbon solubility (atom%) at 1000 °C
Co	3.41
Ni	2.03
Cu	0.04
Ru	1.56
Rh	0.89
Pd	5.98
Ag	0.01
Re	4.39
Ir	1.35
Pt	1.76
Au	0.01

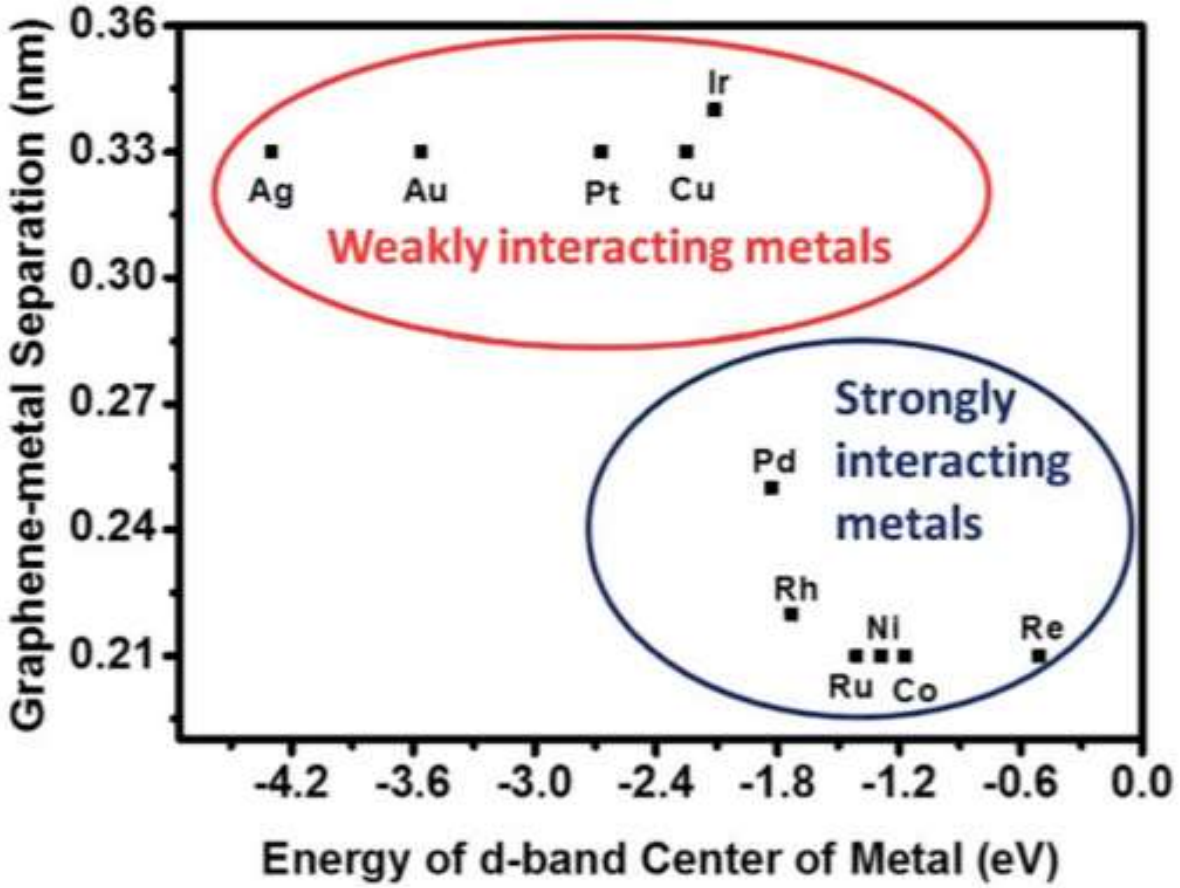
Graphene-metal Separation (nm)
0.36
0.33
0.30
0.27
0.24
0.21
Ag
Au
Pt
Cu
Ir
Weakly interacting metals
Strongly interacting metals
Pd
Rh
Ni
Ru
Co
Re
-4.2
-3.6
-3.0
-2.4
-1.8
-1.2
-0.6
0.0
Energy of d-band Center of Metal (eV)

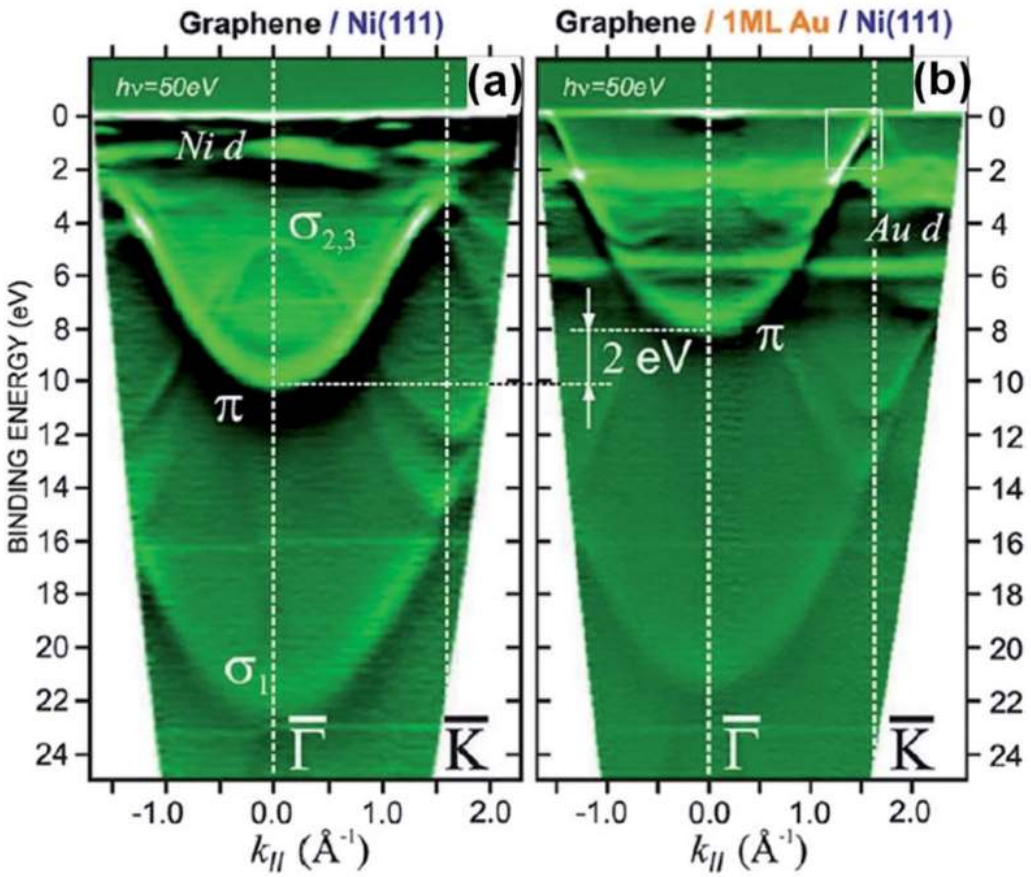
Graphene / Ni(111)
Graphene / 1ML Au / Ni(111)
hν=50eV
hν=50eV
(a)
(b)
Ni d
σ2,3
π
σ1
Au d
2 eV
Γ̄
K̄
Γ̄
K̄
BINDING ENERGY (eV)
0
2
4
6
8
10
12
14
16
18
20
22
24
-1.0
0.0
1.0
2.0
kII (Å-1)
kII (Å-1)

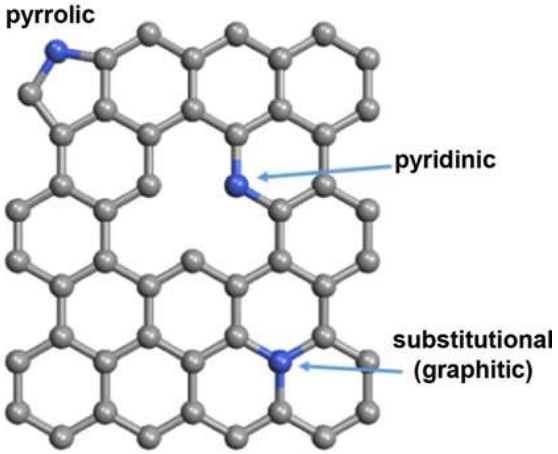

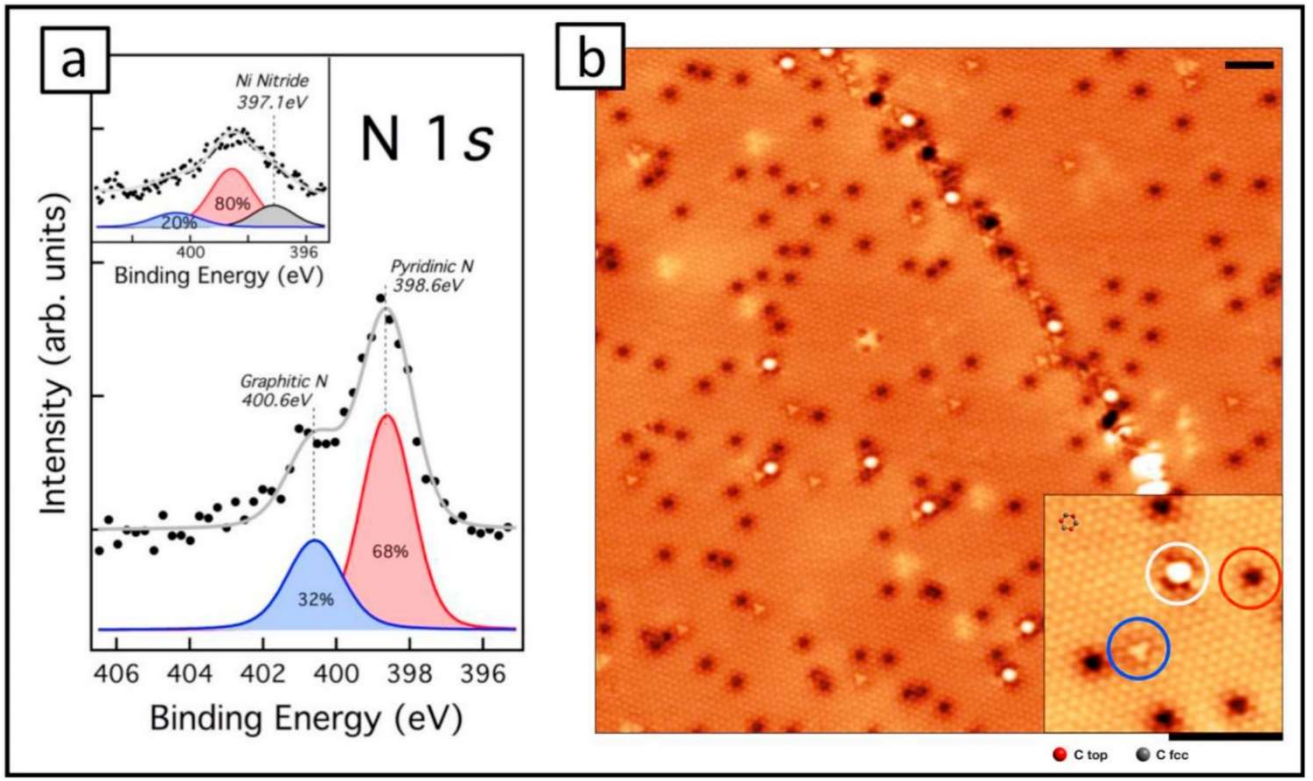

Carbon 171 (2021) 704–710

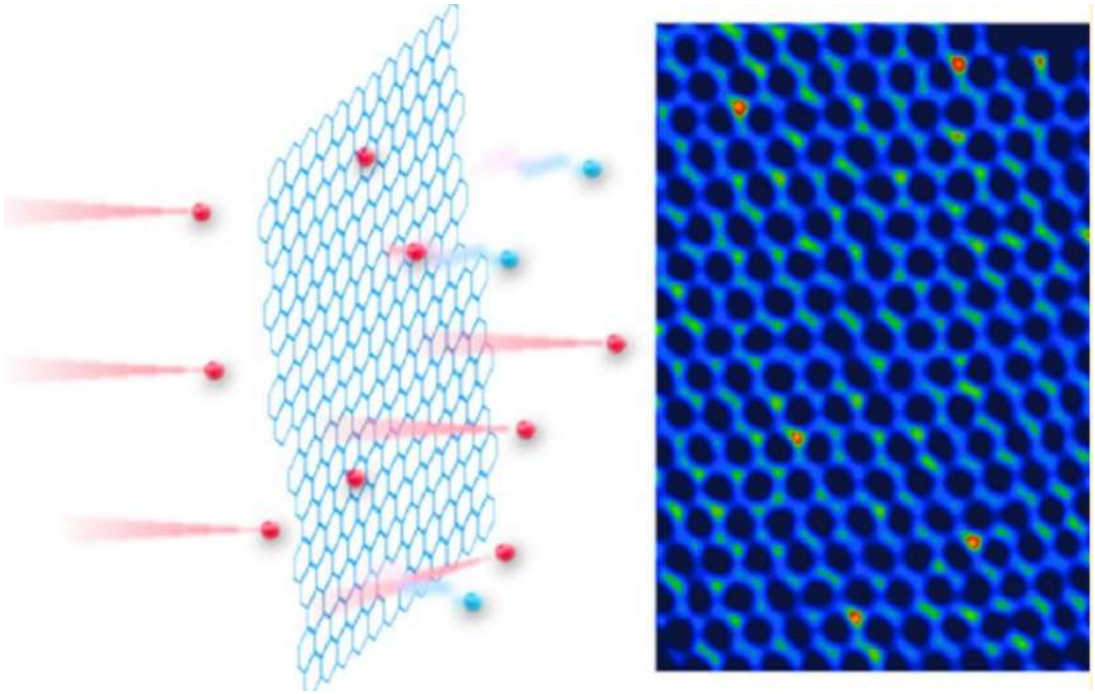

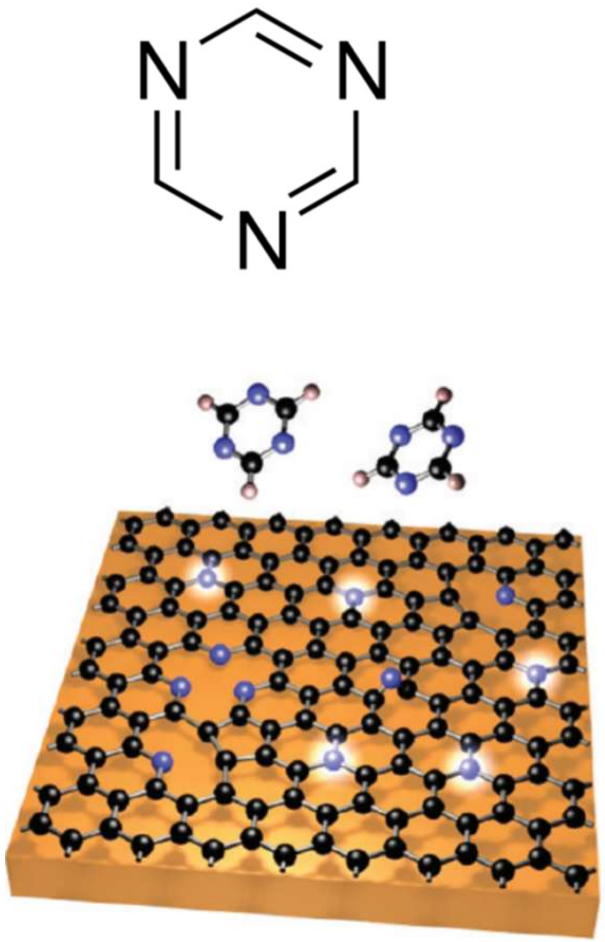

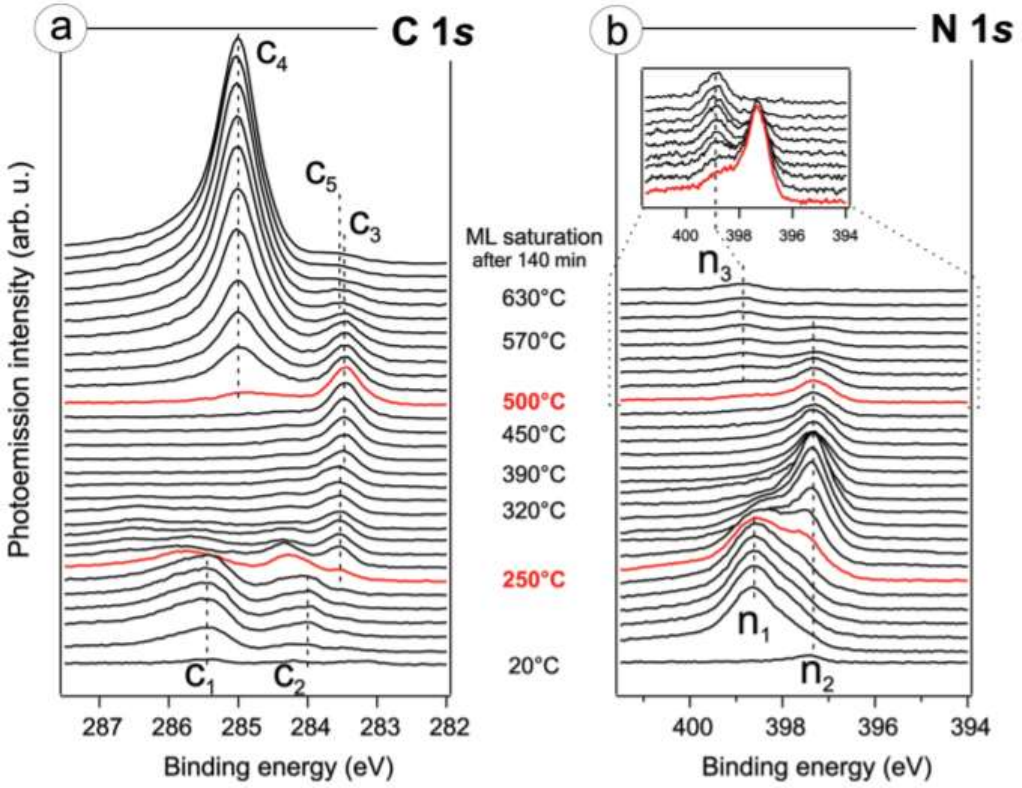

Nano Lett. 2011, 11, 5401–5407

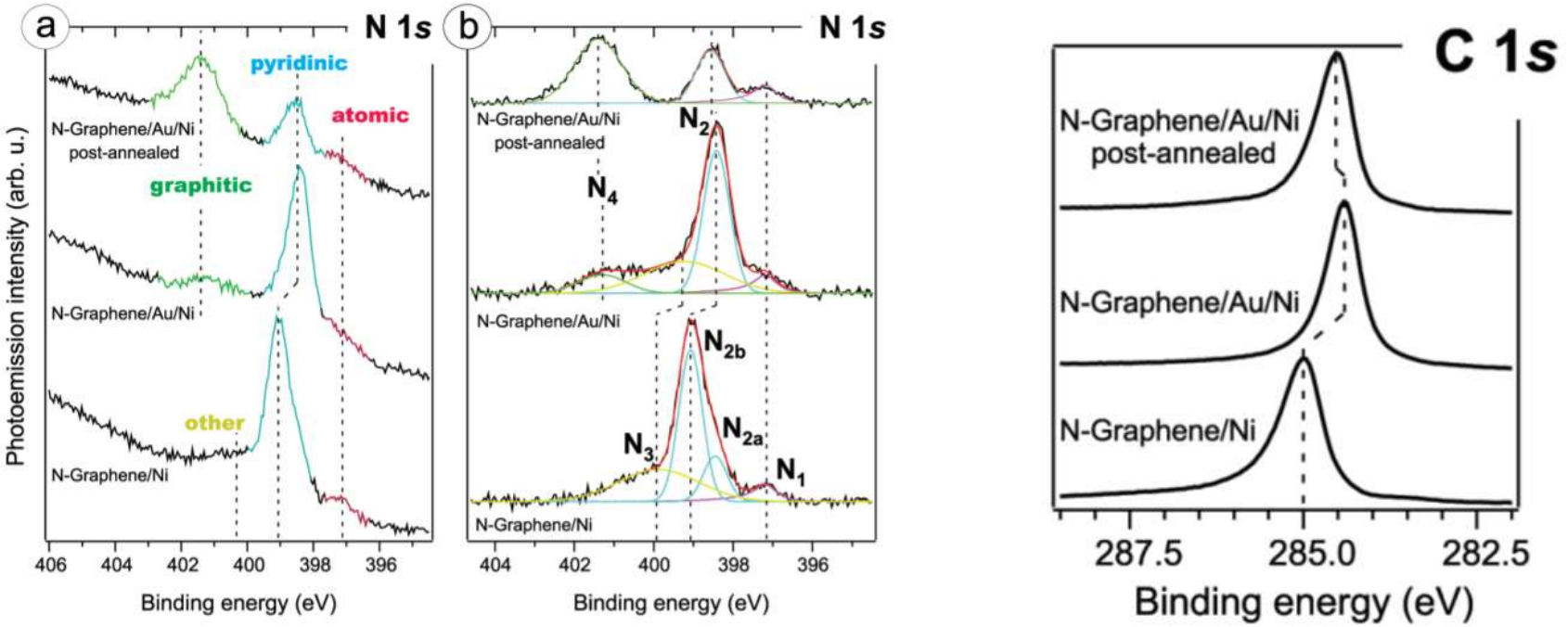

Nano Lett. 2011, 11, 5401–5407

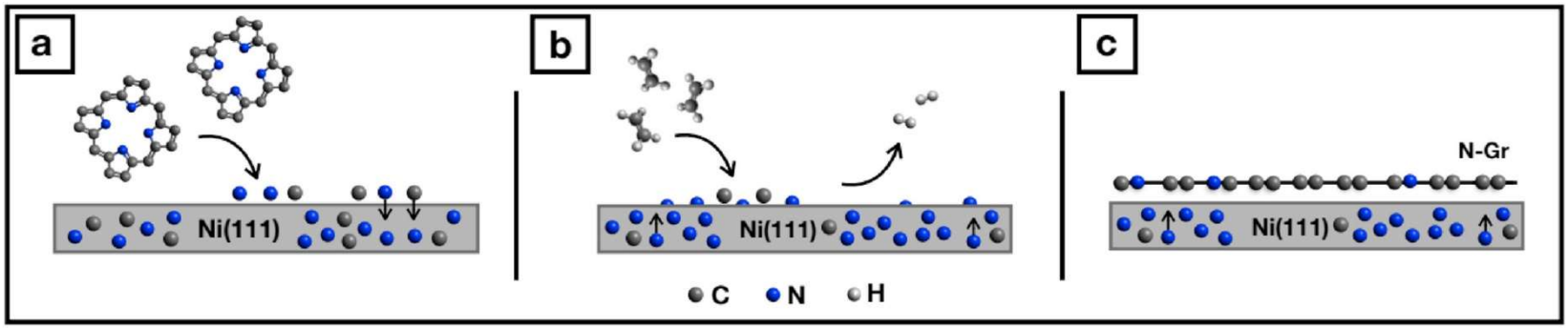

Carbon 171 (2021) 704–710

Naphthylmethyl amine (NMA)

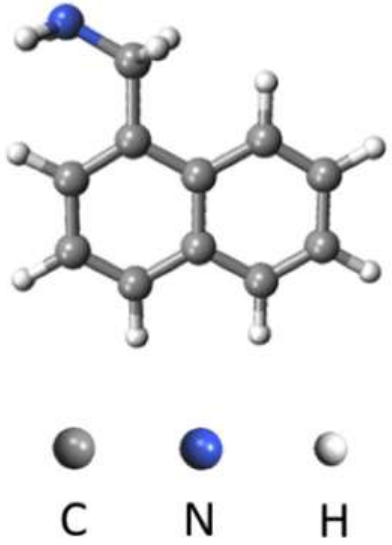

on Au(111)

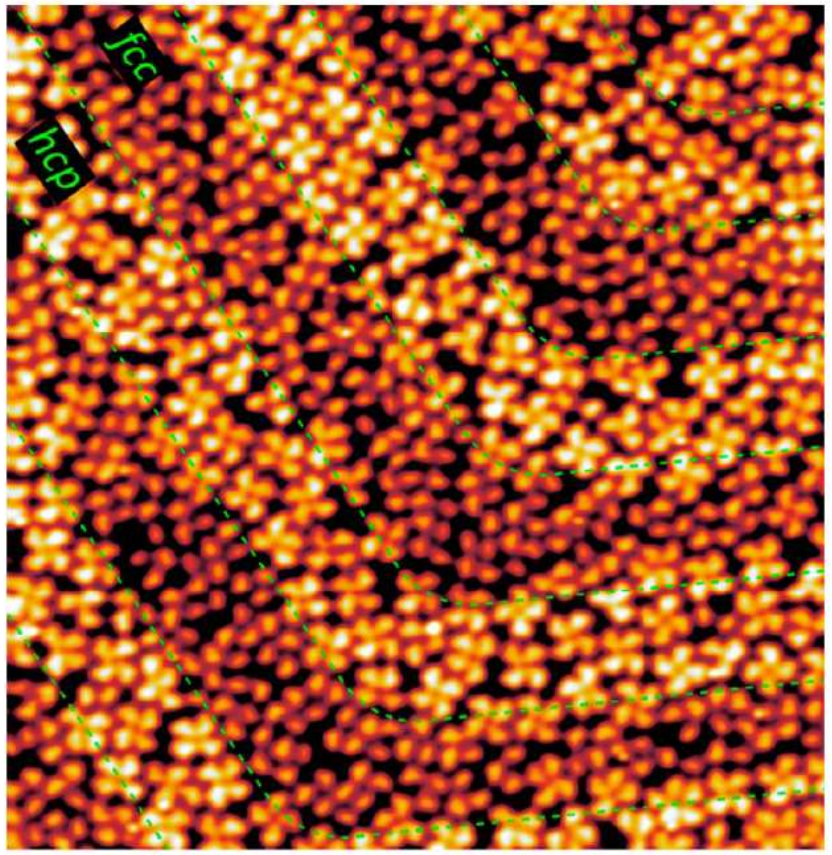

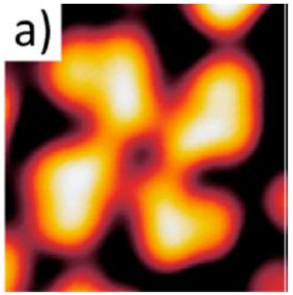

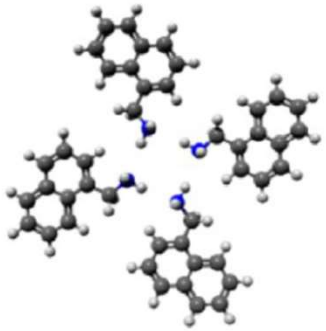

J. Phys. Chem. C 2016, 120, 11, 6104–6115

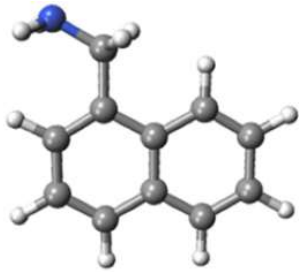

on Au(111)

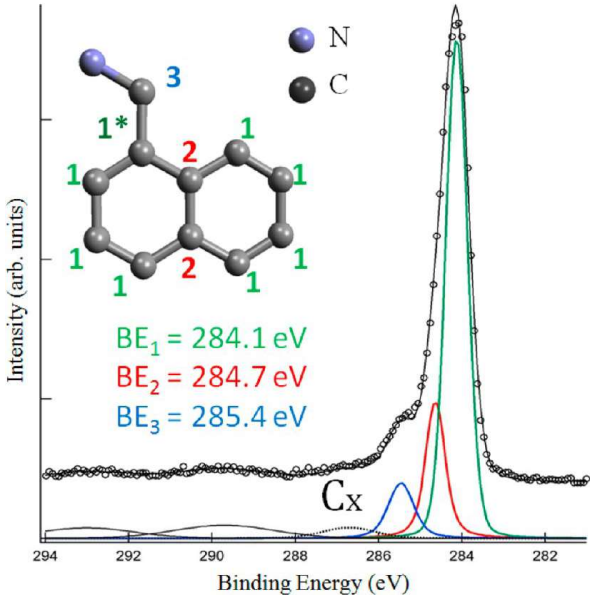
N
C
3
1*
2
1
1
1
1
2
1
1
1
BE1 = 284.1 eV
BE2 = 284.7 eV
BE3 = 285.4 eV
Cx
Intensity (arb. units)
294
292
290
288
286
284
282
Binding Energy (eV)

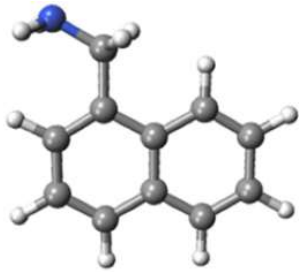

on Ni(111)

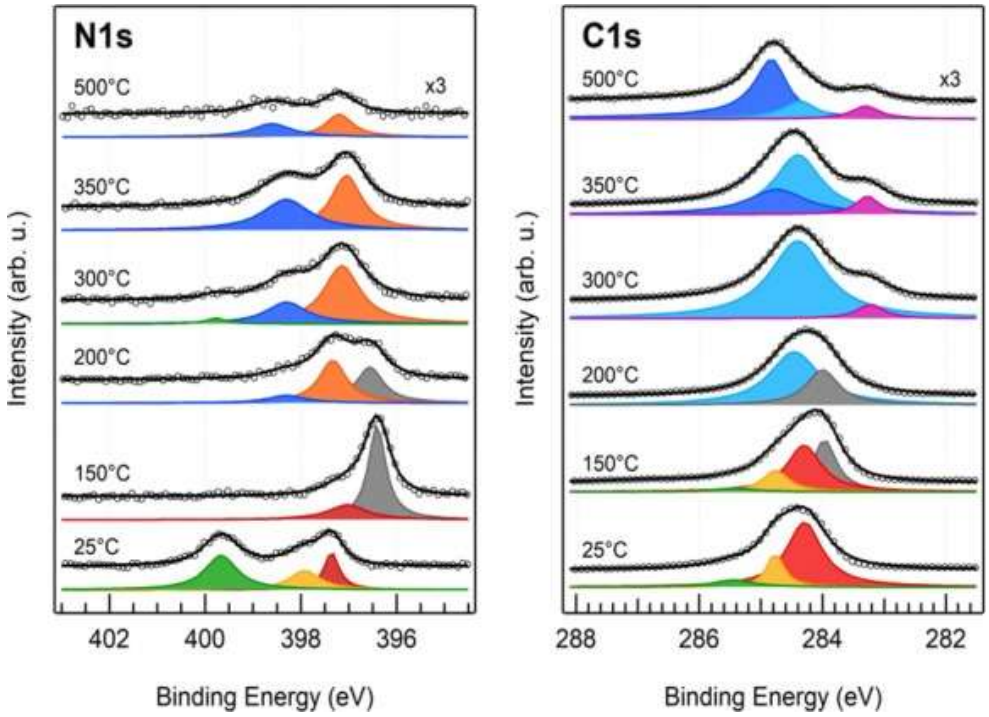

Costantini et al., FlatChem 24 (2020) 100205

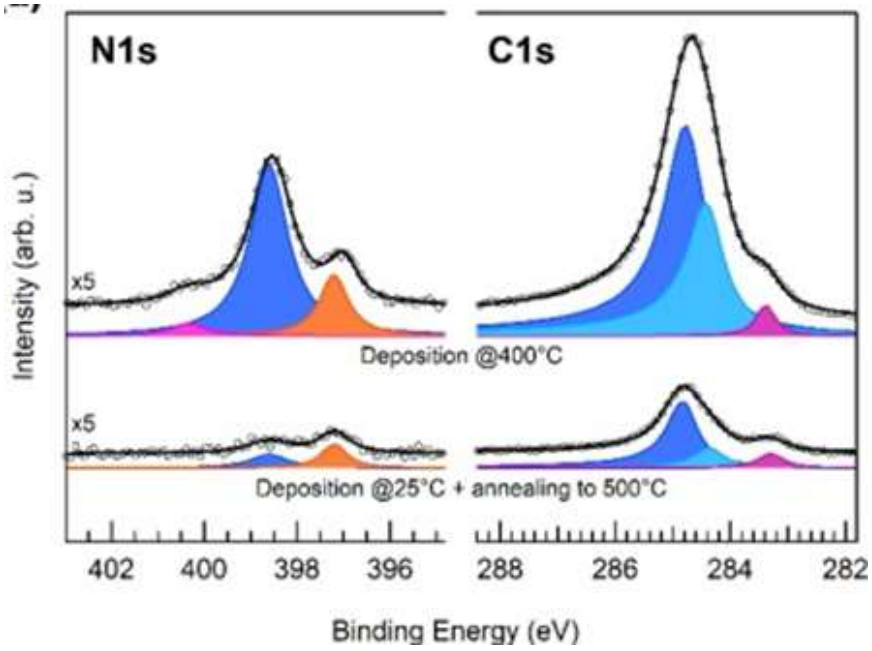

Costantini et al., FlatChem 24 (2020) 100205

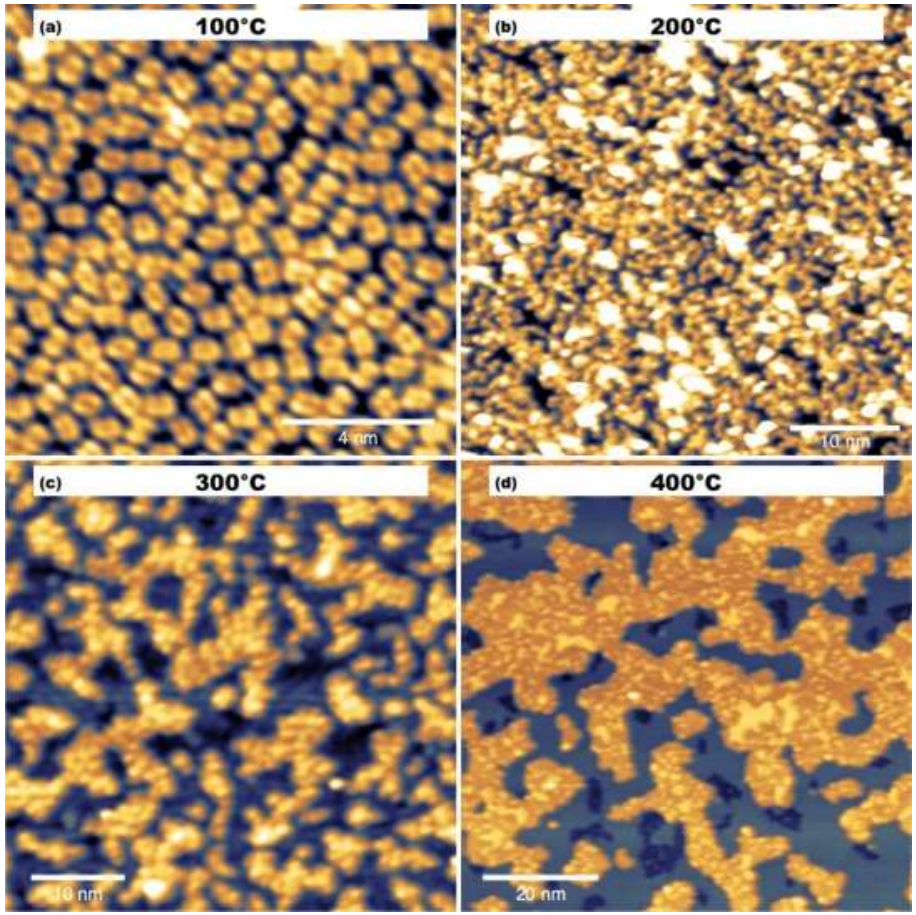

Costantini et al., FlatChem 24 (2020) 100205

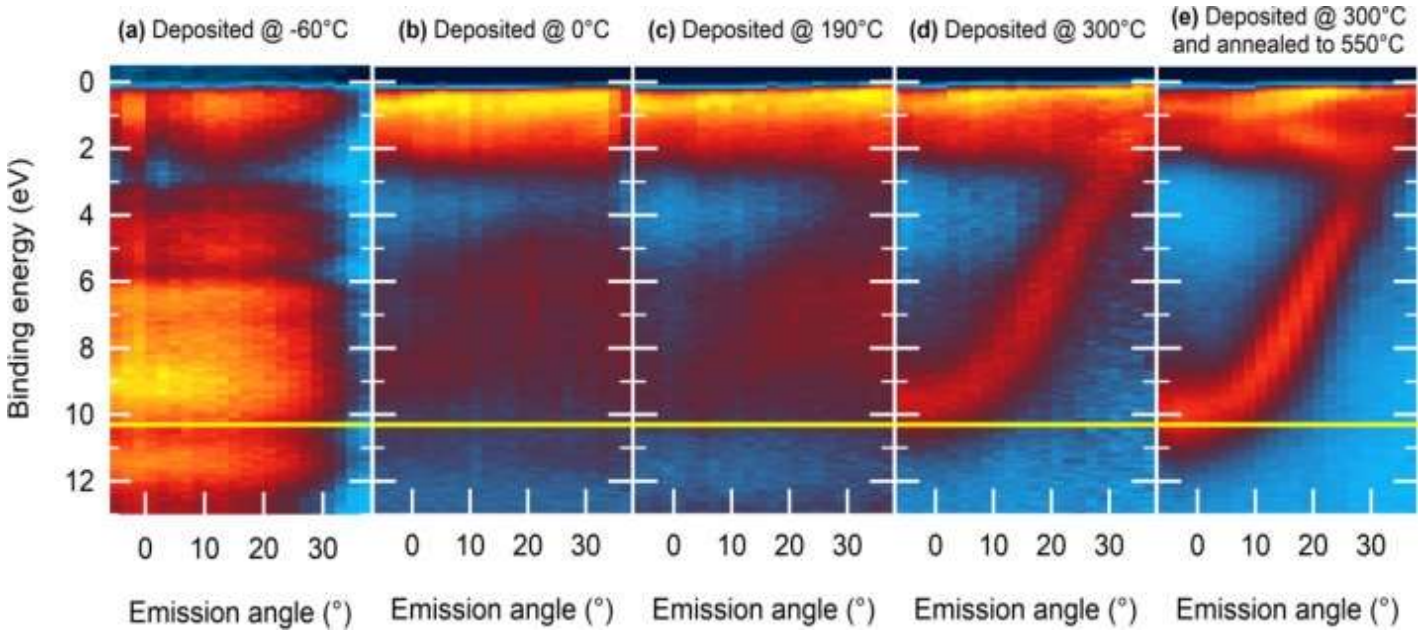

Costantini et al., FlatChem 24 (2020) 100205

Sintesi in sequenza:

1. Ullmann
2. Cyclodehydrogenation

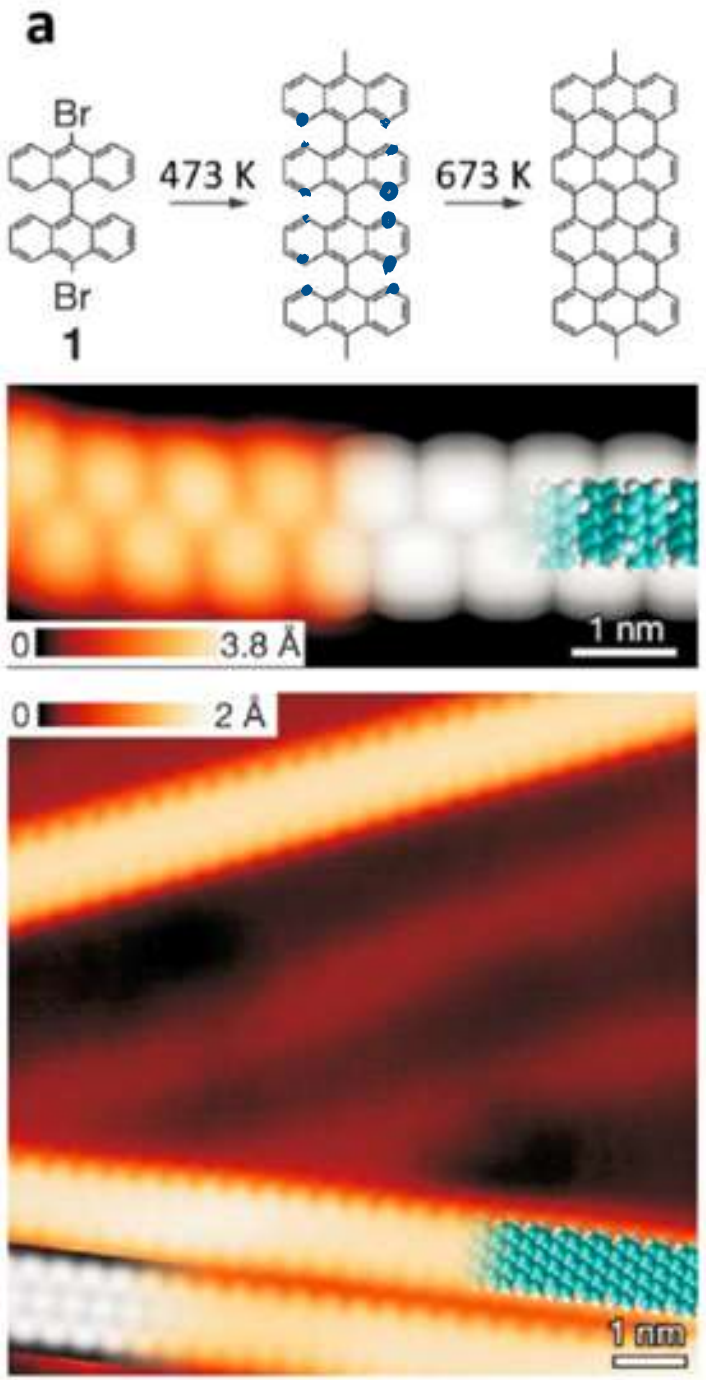

Nature 2010, 466, 470–473

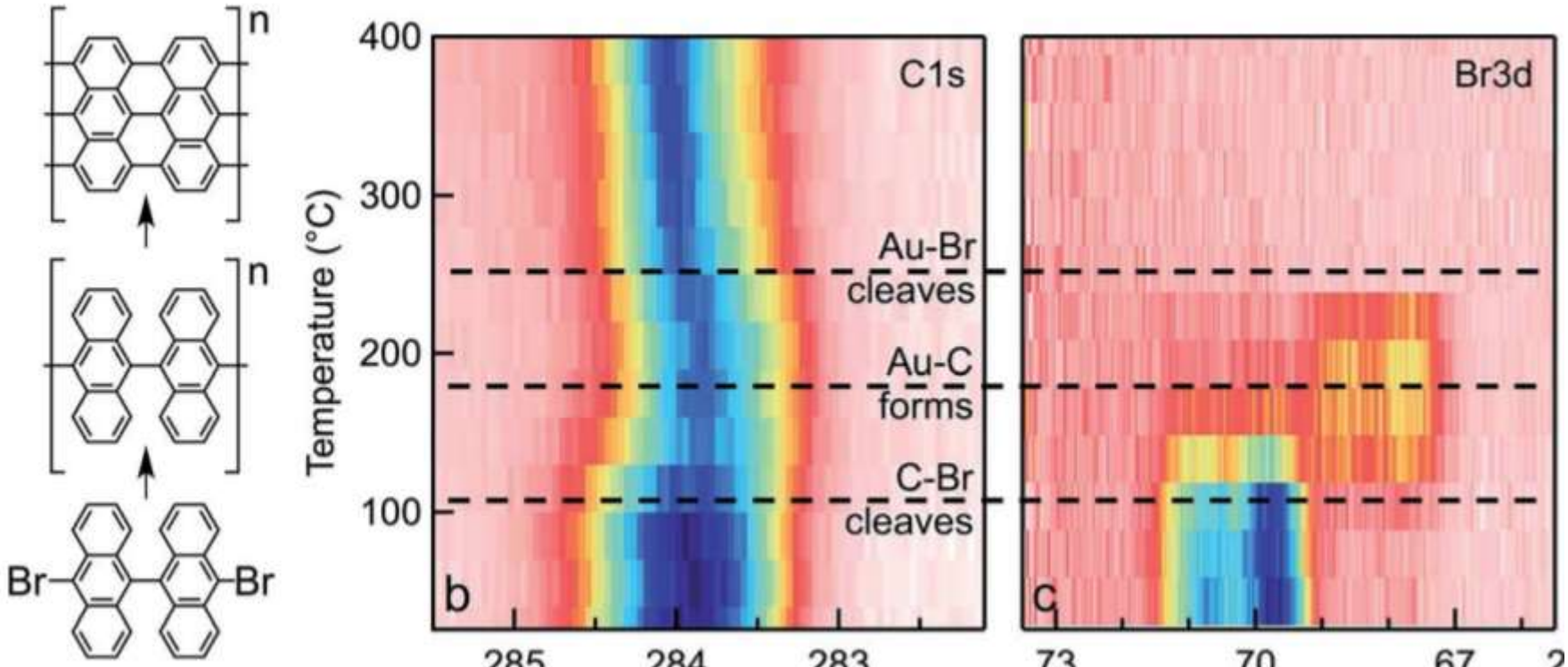

bande électronique E(k)

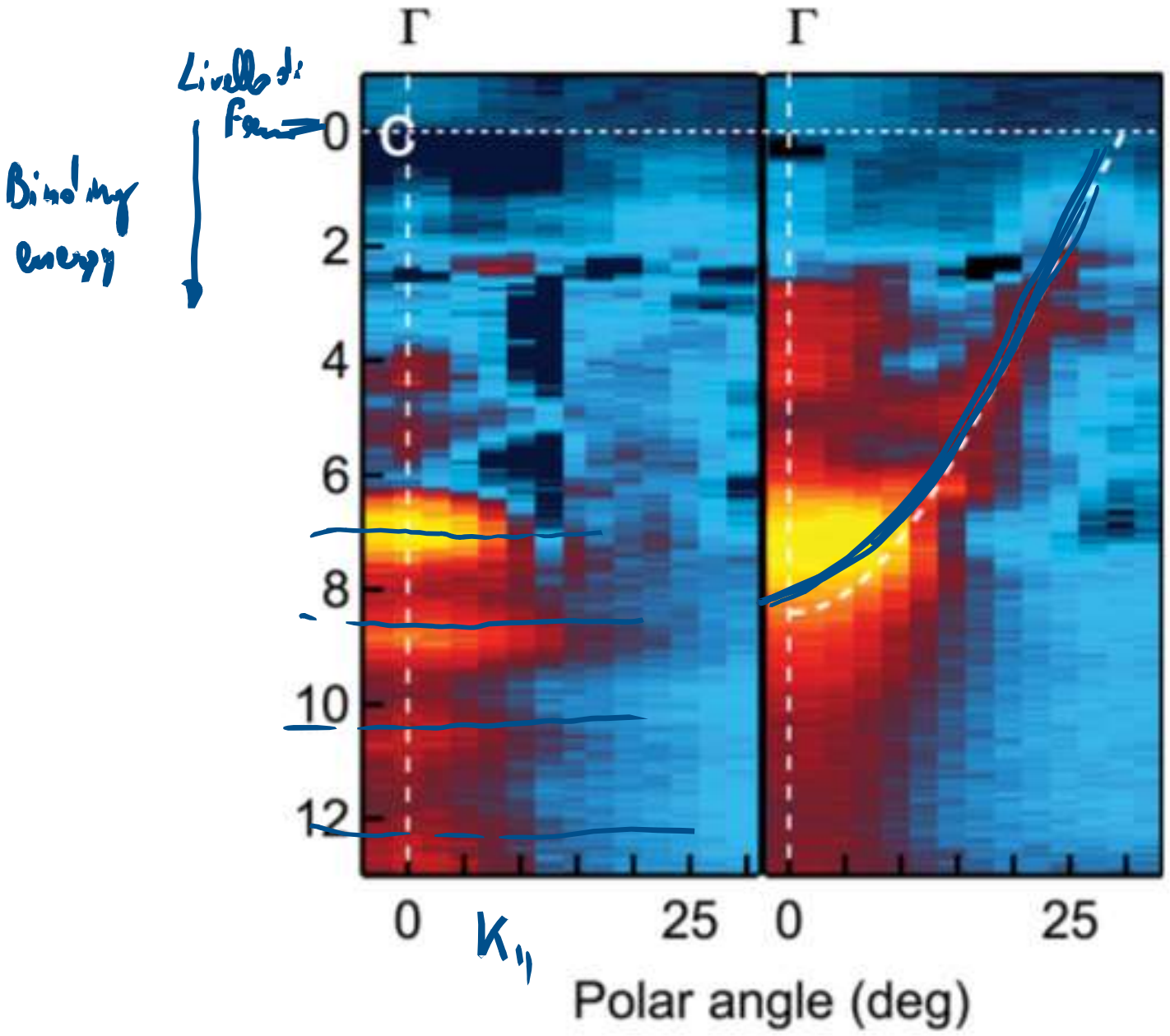
Γ
Γ
Binding energy
0
2
4
6
8
10
12
0
25
0
25
$k_{//}$
Polar angle (deg)